

Ultra-Low-Complexity Algorithms with Structurally Optimal Multi-Group Multicast Beamforming in Large-Scale Systems

Chong Zhang, *Student Member, IEEE*, Min Dong, *Senior Member, IEEE*, and Ben Liang, *Fellow, IEEE*

Abstract—We consider an ultra-low-complexity multi-group multicast beamforming design for large-scale systems. For the quality-of-service (QoS) problem, by utilizing the optimal multicast beamforming structure obtained recently in [2], we convert the original problem into a non-convex weight optimization problem of a lower dimension and propose two fast first-order algorithms to solve it. Both algorithms are based on successive convex approximation (SCA) and provide fast iterative updates to solve each SCA subproblem. The first algorithm uses a saddle point reformulation in the dual domain and applies the extragradient method with an adaptive step-size procedure to find the saddle point with simple closed-form updates. The second algorithm adopts the alternating direction method of multipliers (ADMM) method by converting each SCA subproblem into a favorable ADMM structure. The structure leads to simple closed-form ADMM updates, where the problem in each update block can be further decomposed into parallel subproblems of small sizes, for which closed-form solutions are obtained. We also propose efficient initialization methods to obtain favorable initial points that facilitate fast convergence. Furthermore, taking advantage of the proposed fast algorithms, for the max-min fair (MMF) problem, we propose a simple closed-form scaling scheme that directly uses the solution obtained from the QoS problem, avoiding the conventional computationally expensive method that iteratively solves the inverse QoS problem. We further develop lower and upper bounds on the performance of this scaling scheme. Simulation results show that the proposed algorithms offer near-optimal performance with substantially lower computational complexity than the state-of-the-art algorithms for large-scale systems.

I. INTRODUCTION

Content distribution through wireless multicasting has been increasingly popular among new wireless services and applications and is expected to dominate future wireless traffic. Multi-antenna multicast beamforming is an efficient transmission technique to support high-speed content distribution to multiple user groups simultaneously for future wireless networks. With massive multiple-input multiple-output (MIMO) becoming the essential technology for future networks [3], it is critical for multicast beamforming solutions to be scalable to meet the ultra-low complexity requirement for large-scale systems.

Downlink multicast beamforming has been studied for traditional multi-antenna systems in various scenarios, such as single-group or multi-group multicasting [4]–[6], multi-cell networks [7], [8], relay networks [9], [10], and cognitive radio networks [11], [12]. Multicast beamforming problems are challenging to solve, as they are generally non-convex and NP-hard [4]. Semi-definite relaxation (SDR) has been a prior state-of-the-art method considered in the existing works [13]. For traditional multi-antenna systems with relatively small

problem sizes, SDR provides a good approximate solution [4]–[6], [8]. However, SDR is not a scalable method for large-scale problems, where the computational complexity becomes very high and the performance deteriorates significantly as the problem size grows.

With the increasing number of transmit antennas, successive convex approximation (SCA) [14] has become a more attractive approach to solve the multi-group multicast beamforming problems due to its computational and performance advantages over SDR [15]–[17]. SCA-based methods convexify the non-convex problem into a sequence of convex approximation subproblems, where the convex subproblems are typically solved by the interior-point method (IPM) [18]. However, IPM is a second-order algorithm. For computing a multicast beamforming solution in large-scale massive MIMO systems, using IPM still results in a relatively high computational complexity.

Following this, several methods have been proposed to further reduce the computational complexity at each SCA iteration. For the single-group case, first-order methods have been proposed to solve the convex subproblems [19], [20]. However, these methods are not directly applicable to multiple groups with inter-group interference. For the multi-group scenario with per-antenna power constraints, the alternating direction method of multipliers (ADMM) [21] has been considered for solving the subproblem in each SCA iteration. In [22], zero-forcing pre-processing for interference elimination has been proposed to reduce the multi-group case to a single-group equivalent problem, for which SCA is applied. These methods provide much lower complexity than the original SCA-based method. However, since the dimension of beamforming vectors is dictated by the number of antennas, the computational complexity of these methods still grows with the number of antennas in polynomial time. This renders these methods still computationally costly for massive MIMO systems. Alternatively, for multi-cell systems, low-complexity beamforming schemes using weighted maximum ratio transmission (MRT) in combination with SDR have been developed, where only the weights, one for each user, need to be optimized, and thus the size of the optimization problem is reduced [23], [24]. Despite all the above advancements in computational algorithms, they do not optimally utilize the multicast beamforming structure.

The optimal multi-group multicast beamforming structure has been recently obtained in [2]. It is shown that the optimal solution is a weighted minimum mean-square error (MMSE) filter with an inherent low-dimensional structure for the unknown weights to be computed. With this structure, the multicast beamforming problem can be transformed into a weight optimization problem of a much lower dimension, independent of the number of antennas. As a result, the solution can be computed with significantly lower computational complexity, no longer growing with the number of antennas [2]. Thus, it offers design opportunities for computationally efficient algorithms for

Chong Zhang and Ben Liang are with the Department of Electrical and Computer Engineering, University of Toronto, Canada (e-mail: {chongzhang, liang}@ece.utoronto.ca). Min Dong is with the Department of Electrical, Computer and Software Engineering, Ontario Tech University, Canada (e-mail: min.dong@ontariotechu.ca). Part of this work was presented in [1].

large-scale massive MIMO systems. However, [2] still adopted the conventional IPM-based SCA method for the weight optimization, whose computational complexity still does not scale well with the total number of users. Our goal in this work is to develop scalable first-order fast algorithms for large-scale systems that exploit both the optimal beamforming structure and optimization techniques.

Multicast beamforming problems considered in all the above-mentioned works typically are cast into two problem formulations: a quality-of-service (QoS) problem for transmit power minimization with signal-to-interference-and-noise (SINR) guarantees for all users, or a max-min fair (MMF) problem for maximizing the minimum SINR among all users subject to a transmit power budget. Although both types of problems are non-convex and NP-hard, the MMF problem is more complicated to solve than the QoS problem. Typically, the solution to the MMF problem is obtained through iteratively solving its inverse QoS problem along with a bi-section search over the value of minimum SINR [2], [5], [6], [17], [21]. This additional layer of bi-section iterations results in high computational complexity for the MMF problem in large-scale systems. Therefore, developing a low-complexity method to obtain a good solution for the MMF problem is also critically important.

Besides the above-mentioned works on algorithm development for multicast beamforming design, asymptotic multicast beamforming in massive MIMO systems has been analyzed in [25], [26] without inter-group interference consideration, and in [2] with inter-group interference consideration. Multicast beamforming has also been investigated for energy efficiency maximization [27] and for joint unicast and multicast transmission in massive MIMO systems [28], [29]. For overloaded systems with fewer antennas than the users, the rate-splitting-based multicast beamforming strategies have been proposed [30]–[32]. These studies address different problems from the one considered in our work.

A. Contributions

In this paper, for downlink multi-group multicast beamforming, we propose two fast first-order algorithms for the QoS problem in large-scale massive MIMO systems, which are scalable in both antenna and user dimensions. Utilizing the optimal multicast beamforming structure, we convert the original QoS problem into a non-convex weight optimization problem of a lower dimension. We then develop two fast algorithms to solve this weight optimization problem to obtain our multicast beamforming solution. The two algorithms are SCA-based methods, referred to as the extragradient-based SCA (ESCA) and ADMM-based SCA (ASCA). Using these algorithms, we also propose a simple closed-form scaling scheme for solving the MMF problem. The main novelties and contributions of this work are summarized as follows:

- We first propose ESCA to solve each SCA subproblem in the dual domain. In particular, we construct a saddle point reformulation of the dual problem, which can be further cast as a variational inequality problem where we apply the extragradient method to find the saddle point. The advantage of our approach is that by computing the gradient of the Lagrangian in the dual domain, we obtain simple closed-form gradient updates in each updating step, which is the key for our algorithm to obtain a solution efficiently. To avoid the

need to find the Lipschitz constant of the gradient function, which is generally difficult to obtain, we adopt a prediction-correction procedure for an adaptive step size in each update to ensure convergence to the saddle point to obtain the optimal solution. We also consider two initialization methods, a fast extragradient-based initialization method and an SDR-based method, for generating favorable initial feasible points for ESCA to facilitate fast convergence.

- We also propose a fast ADMM-based algorithm for the SCA subproblems, referred to as ASCA. We transform each SCA subproblem into a favorable form for the ADMM procedure with three updating blocks. In particular, the structure of the transformed problem leads to simple updates in each ADMM update block, where the problem in each update block can be further decomposed into parallel subproblems of small sizes, for each of which a closed-form solution is obtained. Thus, ASCA takes advantage of the closed-form updates in the ADMM procedure for fast computation and is guaranteed to converge to the optimal solution. In addition, a fast ADMM-based fast initialization method is also considered to facilitate fast convergence of the algorithm.
- Taking advantage of the proposed fast algorithms for the QoS problems, we propose a simple closed-form scaling scheme to obtain a multicast beamforming solution for the MMF problem. The scheme directly scales the beamforming solution obtained from the QoS problem to meet the transmit power budget. It thus has substantially lower computational complexity than the conventional method of iteratively solving the inverse QoS problem with bi-section search. We also provide lower and upper bounds on the performance of the scaling scheme.
- Simulation results demonstrate the fast convergence of our proposed ESCA and ASCA with the initialization methods. Both algorithms provide near-optimal performance for the QoS problem. The scalability of our algorithms for large-scale systems is demonstrated, where the computational complexity is substantially lower than the state-of-the-art algorithms for large-scale systems as the number of antennas and users increases. In addition, the proposed scaling scheme for the MMF problem is shown to result in only a mild loss to the optimal performance as the number of antennas becomes large but substantially faster to compute the solution.

B. Organization and Notations

The rest of this paper is organized as follows. Section II presents the system model and problem formulation for multi-group multicast beamforming. Section III reviews the optimal multicast beamforming structure and the SCA method. In Sections IV and V, we present two fast algorithms, ESCA and ASCA, for the QoS problem. In Section VI, we propose a simple closed-form scaling scheme to find the solution for the MMF problem. Simulation results are provided in Section VII, and the conclusion is presented in Section VIII.

Notations: Hermitian, transpose, and conjugate are denoted as $(\cdot)^H$, $(\cdot)^T$, and $(\cdot)^*$, respectively. The real and imaginary parts of a complex number are denoted as $\Re\{\cdot\}$ and $\Im\{\cdot\}$, respectively. The Euclidean norm of a vector is denoted as $\|\cdot\|$. The notation $\mathbf{x} \succeq \mathbf{0}$ indicates element-wise non-negative. The identity matrix is denoted as \mathbf{I} . The notation $\mathbf{z} \sim \mathcal{CN}(\mathbf{0}, \mathbf{C})$ means \mathbf{z} is a complex Gaussian random vector with zero mean

and covariance \mathbf{C} . The non-negative real Euclidean space is denoted as \mathbb{R}_+ .

II. SYSTEM MODEL AND PROBLEM FORMULATION

We consider a downlink multi-group multicast beamforming scenario, where the base station (BS) equipped with N antennas provides service for G user groups. Each group receives a common message that is independent of the messages to other groups. Denote the set of group indices by $\mathcal{G} \triangleq \{1, \dots, G\}$. Assume that there are K_i single-antenna users in group i , and the set of user indices in the group is denoted by $\mathcal{K}_i \triangleq \{1, \dots, K_i\}$, $i \in \mathcal{G}$. Define the total number of users in all groups as $K_{\text{tot}} \triangleq \sum_{i=1}^G K_i$.

Let $\mathbf{h}_{ik} \in \mathbb{C}^{N \times 1}$ be the channel vector from the BS to user k in group i , for $k \in \mathcal{K}_i$, $i \in \mathcal{G}$. Let $\mathbf{w}_i \in \mathbb{C}^{N \times 1}$ be the multicast beamforming vector for group $i \in \mathcal{G}$. The received signal at user k in group i is given by

$$y_{ik} = \mathbf{w}_i^H \mathbf{h}_{ik} s_i + \sum_{j \neq i} \mathbf{w}_j^H \mathbf{h}_{ik} s_j + n_{ik}$$

where s_i is the data symbol transmitted to group i with $E(|s_i|^2) = 1$, and n_{ik} is the receiver additive white Gaussian noise with zero mean and variance σ^2 . The received SINR at user k in group i is expressed as

$$\text{SINR}_{ik} = \frac{|\mathbf{w}_i^H \mathbf{h}_{ik}|^2}{\sum_{j \neq i} |\mathbf{w}_j^H \mathbf{h}_{ik}|^2 + \sigma^2}.$$

The transmit power at the BS is given by $P_t \triangleq \sum_{i=1}^G \|\mathbf{w}_i\|^2$.

Two types of problem formulations are typically considered for the multicast beamforming design. The QoS problem is to minimize the transmit power while meeting the received SINR target at each user, which is formulated as

$$\mathcal{P}_o : \min_{\mathbf{w}} \sum_{i=1}^G \|\mathbf{w}_i\|^2 \quad \text{s.t.} \quad \text{SINR}_{ik} \geq \gamma_{ik}, \quad k \in \mathcal{K}_i, i \in \mathcal{G} \quad (1)$$

where $\mathbf{w} \triangleq [\mathbf{w}_1^H, \dots, \mathbf{w}_G^H]^H$, and γ_{ik} is the SINR target for user k in group i . The other problem formulation is the (weighted) MMF problem, which is to maximize the minimum (weighted) SINR among all users subject to the transmit power constraint at the BS:

$$\mathcal{S}_o : \max_{\mathbf{w}} \min_{i,k} \frac{\text{SINR}_{ik}}{\gamma_{ik}} \quad \text{s.t.} \quad \sum_{i=1}^G \|\mathbf{w}_i\|^2 \leq P \quad (2)$$

where P is the transmit power budget at the BS, and $\{\gamma_{ik}\}$ here serve as the weights to control the grade of service or fairness among users. It is well-known that both \mathcal{P}_o and \mathcal{S}_o are non-convex and NP-hard. The existing works have proposed various computational optimization methods to find good suboptimal solutions. We will first focus on the QoS problem \mathcal{P}_o and develop two fast first-order algorithms to obtain the solutions for \mathcal{P}_o . Then, we discuss how to use the proposed algorithms to solve the MMF problem efficiently.

III. OPTIMAL MULTICAST BEAMFORMING STRUCTURE AND THE SCA METHOD

The optimal multicast beamforming structure has been obtained recently in [2]. Under this structure, problem \mathcal{P}_o is transformed into an equivalent weight optimization problem of

a much lower dimension that is independent of the number of antennas. This leads to a significant computational saving and provides opportunities for efficient algorithm designs for massive MIMO systems. To facilitate our algorithm development later, we briefly describe the optimal multicast beamforming structure obtained in [2], the transformed weight optimization problem, and the SCA method for the problem.

A. Optimal Multicast Beamforming Structure

It is shown in [2] that the optimal solution to \mathcal{P}_o is a weighted MMSE filter given by

$$\mathbf{w}_i^o = \mathbf{R}^{-1}(\boldsymbol{\lambda}^o) \mathbf{H}_i \mathbf{a}_i^o, \quad i \in \mathcal{G} \quad (3)$$

where $\mathbf{H}_i \triangleq [\mathbf{h}_{i1}, \dots, \mathbf{h}_{iK_i}] \in \mathbb{C}^{N \times K_i}$ is the channel matrix for group i , $\mathbf{a}_i^o \in \mathbb{C}^{K_i \times 1}$ is the optimal weight vector for group i , and $\mathbf{R}(\boldsymbol{\lambda}^o) \triangleq \mathbf{I} + \sum_{i=1}^G \sum_{k=1}^{K_i} \lambda_{ik}^o \gamma_{ik} \mathbf{h}_{ik} \mathbf{h}_{ik}^H \in \mathbb{C}^{N \times N}$ is the (normalized) noise plus weighted channel covariance matrix, with $\boldsymbol{\lambda}^o \in \mathbb{R}^{K_{\text{tot}} \times 1}$ containing the optimal Lagrangian multipliers $\{\lambda_{ik}^o\}$ associated with the SINR constraints in (1). The k th weight element a_{ik}^o in \mathbf{a}_i^o indicates the relative significance of user k 's channel \mathbf{h}_{ik} in the overall group-channel direction $\mathbf{H}_i \mathbf{a}_i^o$.

To determine \mathbf{w}^o in (3), we need to numerically compute both $\boldsymbol{\lambda}^o$ and $\{\mathbf{a}_i^o\}$. The parameter $\boldsymbol{\lambda}^o$ can be approximately computed by the simple fixed-point iterative method proposed in [2]. Given $\boldsymbol{\lambda}$, based on the optimal solution structure \mathbf{w}_i^o in (3), the original problem \mathcal{P}_o is transformed into the following equivalent weight optimization problem for $\{\mathbf{a}_i\}$

$$\begin{aligned} \mathcal{P}_1 : \min_{\mathbf{a}} \quad & \sum_{i=1}^G \|\mathbf{C}_i \mathbf{a}_i\|^2 \\ \text{s.t.} \quad & \frac{|\mathbf{a}_i^H \mathbf{f}_{iik}|^2}{\sum_{j \neq i} |\mathbf{a}_j^H \mathbf{f}_{jik}|^2 + \sigma^2} \geq \gamma_{ik}, \quad k \in \mathcal{K}_i, i \in \mathcal{G} \end{aligned} \quad (4)$$

where $\mathbf{a} \triangleq [\mathbf{a}_1^H, \dots, \mathbf{a}_G^H]^H$, $\mathbf{C}_i \triangleq \mathbf{R}^{-1}(\boldsymbol{\lambda}) \mathbf{H}_i \in \mathbb{C}^{N \times K_i}$, $\mathbf{f}_{jik} \triangleq \mathbf{C}_j^H \mathbf{h}_{ik} \in \mathbb{C}^{K_j \times 1}$, $k \in \mathcal{K}_i$, $i, j \in \mathcal{G}$. Different from the original problem \mathcal{P}_o with GN variables, the converted problem \mathcal{P}_1 has K_{tot} variables, which does not depend on the number of antennas N . The problem dimension of \mathcal{P}_1 is much smaller than that of \mathcal{P}_o in massive MIMO systems with $K_i \ll N$. The inherent structure of the optimal multicast beamforming solution in (3) paves the way for developing low-complexity fast algorithms for multicast beamforming design in large-scale massive MIMO systems.

B. Obtaining Weights $\{\mathbf{a}_i\}$ via SCA

The weight optimization problem \mathcal{P}_1 is still a non-convex NP-hard problem. The SCA method can be adopted to solve \mathcal{P}_1 , which is guaranteed to converge to the local minimum [14]. Specifically, given any auxiliary vector $\mathbf{v}_i \in \mathbb{C}^{K_i \times 1}$, $i \in \mathcal{G}$, based on the inequality $(\mathbf{a}_i - \mathbf{v}_i)^H \mathbf{f}_{iik} \mathbf{f}_{iik}^H (\mathbf{a}_i - \mathbf{v}_i) \geq 0$, we have $|\mathbf{a}_i^H \mathbf{f}_{iik}|^2 \geq 2\Re\{\mathbf{a}_i^H \mathbf{f}_{iik} \mathbf{f}_{iik}^H \mathbf{v}_i\} - |\mathbf{v}_i^H \mathbf{f}_{iik}|^2$. Replacing the numerator of the SINR expression in (4) by the right-hand side (RHS) of the above inequality, we convexify the SINR constraint and change \mathcal{P}_1 to the following convex optimization problem

$$\begin{aligned} \mathcal{P}_{1\text{SCA}}(\mathbf{v}) : \min_{\mathbf{a}} \quad & \sum_{i=1}^G \|\mathbf{C}_i \mathbf{a}_i\|^2 \\ \text{s.t.} \quad & \gamma_{ik} \sum_{j \neq i} |\mathbf{a}_j^H \mathbf{f}_{jik}|^2 + |\mathbf{v}_i^H \mathbf{f}_{iik}|^2 + \gamma_{ik} \sigma^2 \end{aligned}$$

$$-2\Re\{\mathbf{a}_i^H \mathbf{f}_{iik} \mathbf{f}_{iik}^H \mathbf{v}_i\} \leq 0, \quad k \in \mathcal{K}_i, i \in \mathcal{G}$$

where $\mathbf{v} \triangleq [\mathbf{v}_1^H, \dots, \mathbf{v}_G^H]^H$. Note that the solution to $\mathcal{P}_{1\text{SCA}}(\mathbf{v})$ is always feasible to \mathcal{P}_1 . By updating \mathbf{v} with the solution \mathbf{a} to $\mathcal{P}_{1\text{SCA}}(\mathbf{v})$, we iteratively solve $\mathcal{P}_{1\text{SCA}}(\mathbf{v})$ until convergence.

Since $\mathcal{P}_{1\text{SCA}}(\mathbf{v})$ is convex, it can be solved by the IPM methods available through standard convex solvers. However, the IPM method is a second-order algorithm (*i.e.*, based on the Hessian matrix of the objective function), whose computational complexity is $O(K_{\text{tot}}^3)$. Thus, iteratively solving $\mathcal{P}_{1\text{SCA}}(\mathbf{v})$ via the IPM method still incurs relatively high computational complexity for large-scale systems when K_i is large. To address this, for the rest of this paper, we develop two fast first-order algorithms to solve $\mathcal{P}_{1\text{SCA}}(\mathbf{v})$ that maintain a low complexity in computing the solution for large-scale systems.

IV. EXTRAGRADIENT-BASED SCA ALGORITHM

A. Dual Saddle Point Reformulation

For the purpose of computation, we rewrite problem $\mathcal{P}_{1\text{SCA}}(\mathbf{v})$ using the real and imaginary parts of each complex quantity. Define $\mathbf{x}_i \triangleq [\Re\{\mathbf{a}_i\}^T, \Im\{\mathbf{a}_i\}^T]^T$, $\mathbf{y}_i \triangleq [\Re\{\mathbf{v}_i\}^T, \Im\{\mathbf{v}_i\}^T]^T$. Also, define

$$\mathbf{A}_i \triangleq \begin{bmatrix} \Re\{\mathbf{C}_i\} & -\Im\{\mathbf{C}_i\} \\ \Im\{\mathbf{C}_i\} & \Re\{\mathbf{C}_i\} \end{bmatrix}, \quad \tilde{\mathbf{F}}_{jik} \triangleq \begin{bmatrix} \Re\{\mathbf{f}_{jik}\} & -\Im\{\mathbf{f}_{jik}\} \\ \Im\{\mathbf{f}_{jik}\} & \Re\{\mathbf{f}_{jik}\} \end{bmatrix}$$

for $k \in \mathcal{K}_i, i, j \in \mathcal{G}$. Then, we have $\|\mathbf{C}_i \mathbf{a}_i\|^2 = \|\mathbf{A}_i \mathbf{x}_i\|^2$ and $|\mathbf{a}_j^H \mathbf{f}_{jik}|^2 = \|\mathbf{x}_j^T \tilde{\mathbf{F}}_{jik}\|^2 = \mathbf{x}_j^T \mathbf{F}_{jik} \mathbf{x}_j$, where $\mathbf{F}_{jik} \triangleq \tilde{\mathbf{F}}_{jik} \tilde{\mathbf{F}}_{jik}^T$, for $k \in \mathcal{K}_i$ and $j, i \in \mathcal{G}$. Define $\mathbf{x} \triangleq [\mathbf{x}_1^T, \dots, \mathbf{x}_G^T]^T$ and $\mathbf{y} \triangleq [\mathbf{y}_1^T, \dots, \mathbf{y}_G^T]^T$. With these new variables, $\mathcal{P}_{1\text{SCA}}(\mathbf{v})$ can be equivalently expressed as

$$\begin{aligned} \mathcal{P}_{1\text{SCA}}^{\text{r}}(\mathbf{y}) : & \min_{\mathbf{x}} \sum_{i=1}^G \|\mathbf{A}_i \mathbf{x}_i\|^2 \\ \text{s.t. } & \mathbf{y}_i^T \mathbf{F}_{iik} \mathbf{y}_i + \gamma_{ik} \sum_{j \neq i} \mathbf{x}_j^T \mathbf{F}_{jik} \mathbf{x}_j - 2\mathbf{y}_i^T \mathbf{F}_{iik} \mathbf{x}_i + \gamma_{ik} \sigma^2 \leq 0, \\ & k \in \mathcal{K}_i, i \in \mathcal{G}. \quad (5) \end{aligned}$$

We first describe the class of variational inequality problems [33] below.

Definition 1 (Variational Inequality). Given $\mathcal{Z} \subseteq \mathbb{R}^n$ and a mapping $\psi : \mathcal{Z} \rightarrow \mathbb{R}^n$, the variational inequality is to find $\mathbf{z} \in \mathcal{Z}$ satisfying $\psi(\mathbf{z})^T (\mathbf{z}' - \mathbf{z}) \geq 0, \forall \mathbf{z}' \in \mathcal{Z}$. Operator $\psi(\cdot)$ is said to be monotone on \mathcal{Z} if $[\psi(\mathbf{z}) - \psi(\mathbf{z}')]^T (\mathbf{z} - \mathbf{z}') \geq 0, \forall \mathbf{z}, \mathbf{z}' \in \mathcal{Z}$. The problem is monotone if operator $\psi(\cdot)$ is monotone.

The projection methods belong to a class of iterative algorithms that solve the monotone variational inequality problems [33]. At each iteration, a projection method uses the updating step to compute the point (*i.e.*, the value of the optimization variable) and then projects it onto the feasible set of the problem to ensure the updated point is feasible. In general, the projection methods are computationally-cheap when the projection is easy to compute.

Note that $\mathcal{P}_{1\text{SCA}}^{\text{r}}(\mathbf{y})$ is convex and the objective function is differentiable. Let operator $\psi(\mathbf{x})$ be the gradient of the objective function of $\mathcal{P}_{1\text{SCA}}^{\text{r}}(\mathbf{y})$. Following the optimality criterion for a convex optimization problem, $\psi(\mathbf{x})$ is monotone, and thus $\mathcal{P}_{1\text{SCA}}^{\text{r}}(\mathbf{y})$ is a monotone variational inequality problem. However, it is difficult to find a closed-form expression for the projection onto the feasible set of $\mathcal{P}_{1\text{SCA}}^{\text{r}}(\mathbf{y})$. Thus, directly

applying the projection method to solve $\mathcal{P}_{1\text{SCA}}^{\text{r}}(\mathbf{y})$ is not computationally attractive. To overcome this difficulty, we resort to the Lagrange dual problem of $\mathcal{P}_{1\text{SCA}}^{\text{r}}(\mathbf{y})$.

Define $\phi_{ik}(\mathbf{x}) \triangleq \mathbf{y}_i^T \mathbf{F}_{iik} \mathbf{y}_i + \gamma_{ik} \sum_{j \neq i} \mathbf{x}_j^T \mathbf{F}_{jik} \mathbf{x}_j - 2\mathbf{y}_i^T \mathbf{F}_{iik} \mathbf{x}_i + \gamma_{ik} \sigma^2$ and $\phi_i(\mathbf{x}) \triangleq [\phi_{i1}(\mathbf{x}), \dots, \phi_{iK_i}(\mathbf{x})]^T$, for $k \in \mathcal{K}_i, i \in \mathcal{G}$. The Lagrangian of $\mathcal{P}_{1\text{SCA}}^{\text{r}}(\mathbf{y})$ is given by

$$\mathcal{L}(\mathbf{x}, \boldsymbol{\eta}) = \sum_{i=1}^G (\|\mathbf{A}_i \mathbf{x}_i\|^2 + \boldsymbol{\eta}_i^T \phi_i(\mathbf{x})) \quad (6)$$

where $\eta_{ik} \geq 0$ is the dual variable associated with constraint (5), and $\boldsymbol{\eta} \triangleq [\boldsymbol{\eta}_1^T, \dots, \boldsymbol{\eta}_G^T]^T$ with $\boldsymbol{\eta}_i \triangleq [\eta_{i1}, \dots, \eta_{iK_i}]^T$. The Lagrange dual problem of $\mathcal{P}_{1\text{SCA}}^{\text{r}}(\mathbf{y})$ is given by

$$\mathcal{D}_{1\text{SCA}}^{\text{r}}(\mathbf{y}) : \max_{\boldsymbol{\eta} \geq 0} \min_{\mathbf{x}} \sum_{i=1}^G (\|\mathbf{A}_i \mathbf{x}_i\|^2 + \boldsymbol{\eta}_i^T \phi_i(\mathbf{x})).$$

Let \mathbf{x}^o and $\boldsymbol{\eta}^o$ be the primal and dual optimal solutions for $\mathcal{P}_{1\text{SCA}}^{\text{r}}(\mathbf{y})$. Since $\mathcal{P}_{1\text{SCA}}^{\text{r}}(\mathbf{y})$ is convex and Slater's condition holds, the strong duality holds. It follows that $\mathbf{u}^o \triangleq (\mathbf{x}^o, \boldsymbol{\eta}^o)$ is a saddle point of the Lagrangian $\mathcal{L}(\mathbf{x}, \boldsymbol{\eta})$ [18]. Define operator $g(\mathbf{u})$ as

$$g(\mathbf{u}) = g(\mathbf{x}, \boldsymbol{\eta}) \triangleq \begin{bmatrix} \nabla_{\mathbf{x}} \mathcal{L}(\mathbf{x}, \boldsymbol{\eta}) \\ -\nabla_{\boldsymbol{\eta}} \mathcal{L}(\mathbf{x}, \boldsymbol{\eta}) \end{bmatrix}, \quad \mathbf{u} \in \mathcal{U} \quad (7)$$

where $\mathcal{U} \triangleq \mathbb{R}^{2K_{\text{tot}}} \times \mathbb{R}_+^{K_{\text{tot}}}$ is a closed convex set. Then, $\mathcal{D}_{1\text{SCA}}^{\text{r}}(\mathbf{y})$ can be interpreted as finding the saddle point \mathbf{u}^o . It is shown in [33] that the problem of finding the saddle point \mathbf{u}^o can be cast as the variational inequality problem: Find $\mathbf{u}^o \in \mathcal{U}$ that satisfies the following variational inequality

$$g(\mathbf{u}^o)^T (\mathbf{u} - \mathbf{u}^o) \geq 0, \quad \forall \mathbf{u} \in \mathcal{U}. \quad (8)$$

B. Extragradient-Based SCA

To solve problem (8), one may consider the basic projection algorithm (BPA) [33], which iteratively updates \mathbf{u} using $g(\mathbf{u})$ and then projects it onto \mathcal{U} . However, the convergence of BPA requires operator $g(\mathbf{u})$ to be strongly monotone [33]. Following Definition 1, operator $\psi(\cdot)$ is said to be strongly monotone on \mathcal{Z} , if there exists a constant $c > 0$ such that $[\psi(\mathbf{z}) - \psi(\mathbf{z}')]^T (\mathbf{z} - \mathbf{z}') \geq c \|\mathbf{z} - \mathbf{z}'\|^2, \forall \mathbf{z}, \mathbf{z}' \in \mathcal{Z}$. Since $\mathcal{L}(\mathbf{x}, \boldsymbol{\eta})$ is linear with respect to (w.r.t.) $\boldsymbol{\eta}$, operator $g(\mathbf{u})$ is not strongly monotone on \mathcal{U} . Thus, we cannot apply BPA to our problem due to no convergence guarantee.

Instead of BPA, in this work, we adopt the extragradient algorithm, a variant of BPA, proposed by Korpelevich in [34]. Compared with BPA, the extragradient algorithm can guarantee convergence for a monotone operator, at the cost of an extra update-and-projection step at each iteration. For operator $g(\mathbf{u})$ in (7), since $\mathcal{L}(\mathbf{x}, \boldsymbol{\eta})$ is convex in $\mathbf{x} \in \mathbb{R}^{2K_{\text{tot}}}$ and $-\mathcal{L}(\mathbf{x}, \boldsymbol{\eta})$ is convex in $\boldsymbol{\eta} \in \mathbb{R}_+^{K_{\text{tot}}}$, $g(\mathbf{u})$ is monotone on \mathcal{U} by Definition 1. Thus, we develop a fast iterative algorithm to solve $\mathcal{P}_{1\text{SCA}}^{\text{r}}(\mathbf{y})$ by applying the extragradient algorithm in the problem dual domain.

The updating procedure of the extragradient algorithm for finding the saddle point is summarized as follows [33], [34]: At iteration $n + 1$,

$$\mathbf{x}^{(n+\frac{1}{2})} = \mathbf{x}^{(n)} - \alpha \nabla_{\mathbf{x}^{(n)}} \mathcal{L}(\mathbf{x}^{(n)}, \boldsymbol{\eta}^{(n)}), \quad (9)$$

$$\boldsymbol{\eta}^{(n+\frac{1}{2})} = [\boldsymbol{\eta}^{(n)} + \alpha \nabla_{\boldsymbol{\eta}^{(n)}} \mathcal{L}(\mathbf{x}^{(n)}, \boldsymbol{\eta}^{(n)})]^+, \quad (10)$$

$$\mathbf{x}^{(n+1)} = \mathbf{x}^{(n)} - \alpha \nabla_{\mathbf{x}^{(n+\frac{1}{2})}} \mathcal{L}(\mathbf{x}^{(n+\frac{1}{2})}, \boldsymbol{\eta}^{(n+\frac{1}{2})}), \quad (11)$$

$$\boldsymbol{\eta}^{(n+1)} = [\boldsymbol{\eta}^{(n)} + \alpha \nabla_{\boldsymbol{\eta}^{(n+\frac{1}{2})}} \mathcal{L}(\mathbf{x}^{(n+\frac{1}{2})}, \boldsymbol{\eta}^{(n+\frac{1}{2})})]^+ \quad (12)$$

where $[\mathbf{z}]^+ \triangleq [[z_1]^+, \dots, [z_n]^+]^T$ with $[z_i]^+ \triangleq \max\{z_i, 0\}$, for $\mathbf{z} \in \mathbb{R}^n$, and α is the step size.

The gradient $\nabla_{\mathbf{x}} \mathcal{L}(\mathbf{x}, \boldsymbol{\eta})$ can be denoted as $\nabla_{\mathbf{x}} \mathcal{L}(\mathbf{x}, \boldsymbol{\eta}) = [\nabla_{\mathbf{x}_1} \mathcal{L}(\mathbf{x}, \boldsymbol{\eta})^T, \dots, \nabla_{\mathbf{x}_G} \mathcal{L}(\mathbf{x}, \boldsymbol{\eta})^T]^T$. From (6), we obtain

$$\begin{aligned} \nabla_{\mathbf{x}_i} \mathcal{L}(\mathbf{x}, \boldsymbol{\eta}) &= 2\mathbf{A}_i^T \mathbf{A}_i \mathbf{x}_i + 2 \left(\sum_{j \neq i} \sum_{k=1}^{K_j} \gamma_{jk} \eta_{jk} \mathbf{F}_{ijk} \right) \mathbf{x}_i \\ &\quad - 2 \left(\sum_{k=1}^{K_i} \eta_{ik} \mathbf{F}_{iik} \right)^T \mathbf{y}_i, \quad i \in \mathcal{G}. \end{aligned} \quad (13)$$

Also from (6), we obtain the gradient $\nabla_{\boldsymbol{\eta}} \mathcal{L}(\mathbf{x}, \boldsymbol{\eta})$ as

$$\nabla_{\boldsymbol{\eta}} \mathcal{L}(\mathbf{x}, \boldsymbol{\eta}) = [\phi_1^T(\mathbf{x}), \dots, \phi_G^T(\mathbf{x})]^T. \quad (14)$$

Substituting the expressions in (13) and (14) into (9)–(12), we obtain the closed-form updates for $\mathbf{x}^{(n+1)}$ and $\boldsymbol{\eta}^{(n+1)}$.

For a monotone variational inequality problem with operator being L -Lipschitz continuous, the extragradient algorithm is guaranteed to converge to the optimal solution, provided that the step size satisfies $\alpha < 1/L$ [33]. Unfortunately, it is difficult to determine Lipschitz constant L for $g(\mathbf{u})$ in our problem. To overcome this difficulty, instead of a constant step size α , we adopt an adaptive strategy based on the prediction-correction procedure [35], [36] to adaptively set the step size $\alpha^{(n)}$ for each iteration.

Given a fixed step size α , the prediction-correction procedure contains two steps at iteration $n+1$:

- 1) Prediction: Obtain $\mathbf{u}^{(n+\frac{1}{2})}$ from (9) and (10) with fixed α . Compute $d_{\mathbf{u}}^{(n)} \triangleq \|\mathbf{u}^{(n+\frac{1}{2})} - \mathbf{u}^{(n)}\|$ and $d_g^{(n)} \triangleq \|g(\mathbf{u}^{(n+\frac{1}{2})}) - g(\mathbf{u}^{(n)})\|$. Compute step size $\hat{\alpha}^{(n)} = c \frac{d_{\mathbf{u}}^{(n)}}{d_g^{(n)}}$, where $c \in (0, 1)$ is a constant.
- 2) Correction: Set $\alpha^{(n)} = \min\{\alpha, \hat{\alpha}^{(n)}\}$ for iteration $n+1$ to update $\mathbf{x}^{(n+1)}$ and $\boldsymbol{\eta}^{(n+1)}$ in (9)–(12).

We now show that the prediction-correction procedure guarantees the extragradient algorithm converges to the saddle point \mathbf{u}^o of problem (8). If we replace α by $\alpha^{(n)}$ in (9)–(12) of the extragradient algorithm, then for any step size sequence $\{\alpha^{(n)}\}$, the following holds [35], [36]

$$\begin{aligned} &\|\mathbf{u}^{(n+1)} - \mathbf{u}^o\|^2 \\ &\leq \|\mathbf{u}^{(n)} - \mathbf{u}^o\|^2 - \|\mathbf{u}^{(n+\frac{1}{2})} - \mathbf{u}^{(n)}\|^2 \left(1 - \left(\alpha^{(n)} \frac{d_g^{(n)}}{d_{\mathbf{u}}^{(n)}} \right)^2 \right). \end{aligned} \quad (15)$$

If we set $\alpha^{(n)}$ as in the correction step of the above prediction-correction procedure, then $\|\mathbf{u}^{(n+1)} - \mathbf{u}^o\| < \|\mathbf{u}^{(n)} - \mathbf{u}^o\|$ and $\{\mathbf{u}^{(n)}\}$ move towards the saddle point \mathbf{u}^o of problem (8). It follows that the algorithm converges to the optimal solution to $\mathcal{P}_{\text{ISCA}}^r(\mathbf{y})$ in each SCA iteration.

Overall, the ESCA algorithm to solve \mathcal{P}_1 is summarized in Algorithm 1. The main computational complexity of ESCA lies in computing the gradients $\nabla_{\mathbf{x}_i} \mathcal{L}(\mathbf{x}, \boldsymbol{\eta})$ in (13) and $\nabla_{\boldsymbol{\eta}} \mathcal{L}(\mathbf{x}, \boldsymbol{\eta})$ in (14). The related matrix-vector computation requires a total of $8G \sum_{i=1}^G K_i^3$ flops at each extragradient iteration. The number of iterations for convergence depends on the problem size K_{tot} . From our experiments, it typically takes 20 ~ 200 iterations for $K_{\text{tot}} = 15 \sim 60$ users for the extragradient algorithm to converge at each SCA iteration.

Remark 1. As mentioned earlier, BPA consists of only one

Algorithm 1 ESCA Algorithm to Solve \mathcal{P}_1

- 1: **Initialization:** Set feasible initial point $\mathbf{y}^{(0)}$. Set α and c . Set $l = 0$.
 - 2: **repeat**
 - 3: // solve $\mathcal{P}_{\text{ISCA}}^r(\mathbf{y}^{(l)})$
 - 4: **Initialization:** $\mathbf{x}^{(0)} = \mathbf{y}^{(l)}$, $\boldsymbol{\eta}^{(0)} = \mathbf{0}$, $n = 0$.
 - 5: **repeat**
 - 6: Compute $\mathbf{x}^{(n+\frac{1}{2})}$ and $\boldsymbol{\eta}^{(n+\frac{1}{2})}$ by (9)(10) using α .
 - 7: Compute $g(\mathbf{u}^{(n+\frac{1}{2})})$ by (13)(14).
 - 8: Compute $d_{\mathbf{u}}^{(n)}$ and $d_g^{(n)}$.
 - 9: *Prediction:* Compute $\hat{\alpha}^{(n)} = c d_{\mathbf{u}}^{(n)} / d_g^{(n)}$.
 - 10: *Correction:* Update step size $\alpha^{(n)} = \min\{\alpha, \hat{\alpha}^{(n)}\}$.
 - 11: **if** $\alpha^{(n)} = \alpha$ **then**
 - 12: Update $\mathbf{x}^{(n+1)}$ and $\boldsymbol{\eta}^{(n+1)}$ by (11)(12).
 - 13: **else**
 - 14: Update $\mathbf{x}^{(n+1)}$ and $\boldsymbol{\eta}^{(n+1)}$ by (9)–(12) using $\alpha^{(n)}$.
 - 15: **end if**
 - 16: $n \leftarrow n + 1$.
 - 17: **until** convergence
 - 18: Set $\mathbf{y}^{(l+1)} = \mathbf{x}^{(n)}$. Set $l \leftarrow l + 1$.
 - 19: **until** convergence
-

update-and-projection step at each iteration (similar to (9)(10)), but requires the operator $g(\mathbf{u})$ to be strongly monotone for convergence. If $g(\mathbf{u})$ is only monotone, the updated point (the same as $\mathbf{u}^{(n+\frac{1}{2})}$ in (9)(10) in iteration $n+1$) may move away from, instead of closer to, the optimal point \mathbf{u}^o at each iteration. Thus, the updating procedure may not converge over iterations. In contrast, the extragradient algorithm adds an extra update-and-projection step as in (11)(12) at each iteration. This extra step can ensure convergence for a monotone operator $g(\mathbf{u})$. Specifically, it is shown in [33] that in iteration $n+1$, after obtaining $\mathbf{u}^{(n+\frac{1}{2})}$ at the first update-and-projection step in (9)(10), a hyperplane $\mathcal{H}^{(n)} \triangleq \{\mathbf{u} \mid g(\mathbf{u}^{(n+\frac{1}{2})})^T (\mathbf{u} - \mathbf{u}^{(n+\frac{1}{2})}) = 0\}$ can be constructed at $\mathbf{u}^{(n+\frac{1}{2})}$ with normal vector $g(\mathbf{u}^{(n+\frac{1}{2})})$. For the monotone operator $g(\mathbf{u})$, it is proven that this hyperplane $\mathcal{H}^{(n)}$ separates the point $\mathbf{u}^{(n)}$ and the optimal point \mathbf{u}^o , where \mathbf{u}^o is in the halfspace in the direction $-g(\mathbf{u}^{(n+\frac{1}{2})})$. The second update-and-projection step in (11)(12) then utilizes $-g(\mathbf{u}^{(n+\frac{1}{2})})$ to update $\mathbf{u}^{(n+1)}$. This ensures that $\mathbf{u}^{(n+1)}$ move towards the optimal point \mathbf{u}^o and thus is closer to \mathbf{u}^o than $\mathbf{u}^{(n)}$ is.

C. Initialization for ESCA

A challenge in using SCA to solve \mathcal{P}_1 is that it requires a feasible initial point satisfying the SINR constraint (4) as $\mathbf{v}^{(0)}$ for $\mathcal{P}_{\text{ISCA}}(\mathbf{v})$ (equivalently $\mathbf{y}^{(0)}$ for $\mathcal{P}_{\text{ISCA}}^r(\mathbf{y})$). It is necessary to generate a feasible initial point with a low computational complexity. Furthermore, a good initial point closer to the (locally) optimal point of \mathcal{P}_1 could accelerate the convergence. Below, we consider two initialization methods for ESCA.

1) *Extragradient-based initialization method (EIM):* Based on the extragradient-based algorithm in Section IV-B, we propose EIM as follows. EIM generates a feasible point by solving the following feasibility problem

$$\begin{aligned} &\mathcal{P}_{\text{1fea}} : \text{Find } \{\mathbf{x}\} \\ &\text{s.t. } \frac{\mathbf{x}_i^T \mathbf{F}_{iik} \mathbf{x}_i}{\sum_{j \neq i} \mathbf{x}_j^T \mathbf{F}_{jik} \mathbf{x}_j + \sigma^2} \geq \gamma_{ik}, \quad k \in \mathcal{K}_i, i \in \mathcal{G} \end{aligned} \quad (16)$$

where \mathbf{x}_i and \mathbf{F}_{jik} are defined at the beginning of Section IV-A, and constraint (16) is an equivalent real representation of constraint (4) in \mathcal{P}_1 based on $|\mathbf{a}_j^H \mathbf{f}_{jik}|^2 = \mathbf{x}_j^T \mathbf{F}_{jik} \mathbf{x}_j$.

We solve $\mathcal{P}_{1\text{fea}}$ by applying the extragradient algorithm with the adaptive step size proposed in Section IV-B. Specifically, the Lagrangian of $\mathcal{P}_{1\text{fea}}$ is given by $\tilde{\mathcal{L}}(\mathbf{x}, \tilde{\boldsymbol{\eta}}) = \sum_{i=1}^G \tilde{\phi}_i^T(\mathbf{x}) \tilde{\boldsymbol{\eta}}_i$, where $\tilde{\boldsymbol{\eta}}_i$ is the dual variable for constraint (16), $\tilde{\boldsymbol{\eta}} \triangleq [\tilde{\boldsymbol{\eta}}_1^T, \dots, \tilde{\boldsymbol{\eta}}_G^T]^T$ with $\tilde{\boldsymbol{\eta}}_i \triangleq [\tilde{\eta}_{i1}, \dots, \tilde{\eta}_{iK_i}]^T$, and $\tilde{\phi}_i(\mathbf{x}) \triangleq [\phi_{i1}(\mathbf{x}), \dots, \phi_{iK_i}(\mathbf{x})]^T$ with $\phi_{ik}(\mathbf{x}) \triangleq \gamma_{ik} \sum_{j \neq i} \mathbf{x}_j^T \mathbf{F}_{jik} \mathbf{x}_j - \mathbf{x}_i^T \mathbf{F}_{iik} \mathbf{x}_i + \gamma_{ik} \sigma^2$, for $k \in \mathcal{K}_i, i \in \mathcal{G}$. The gradient $\nabla_{\mathbf{x}_i} \tilde{\mathcal{L}}(\mathbf{x}, \tilde{\boldsymbol{\eta}})$, for $i \in \mathcal{G}$, is given by

$$\nabla_{\mathbf{x}_i} \tilde{\mathcal{L}}(\mathbf{x}, \tilde{\boldsymbol{\eta}}) = 2 \left(\sum_{j \neq i} \sum_{k=1}^{K_j} \gamma_{jk} \tilde{\eta}_{jk} \mathbf{F}_{ijk} \right)^T \mathbf{x}_i - 2 \left(\sum_{k=1}^{K_i} \tilde{\eta}_{ik} \mathbf{F}_{iik} \right)^T \mathbf{x}_i.$$

Similar to (14), the gradient $\nabla_{\tilde{\boldsymbol{\eta}}} \tilde{\mathcal{L}}(\mathbf{x}, \tilde{\boldsymbol{\eta}})$ is given by $\nabla_{\tilde{\boldsymbol{\eta}}} \tilde{\mathcal{L}}(\mathbf{x}, \tilde{\boldsymbol{\eta}}) = [\tilde{\phi}_1^T(\mathbf{x}), \dots, \tilde{\phi}_G^T(\mathbf{x})]^T$. The updating procedure of the extragradient algorithm in (9)–(12) is then applied for solving $\mathcal{P}_{1\text{fea}}$, with $\boldsymbol{\eta}$, $\nabla_{\mathbf{x}} \mathcal{L}(\mathbf{x}, \boldsymbol{\eta})$, and $\nabla_{\boldsymbol{\eta}} \mathcal{L}(\mathbf{x}, \boldsymbol{\eta})$ being replaced by $\tilde{\boldsymbol{\eta}}$, $\nabla_{\mathbf{x}} \tilde{\mathcal{L}}(\mathbf{x}, \tilde{\boldsymbol{\eta}})$, and $\nabla_{\tilde{\boldsymbol{\eta}}} \tilde{\mathcal{L}}(\mathbf{x}, \tilde{\boldsymbol{\eta}})$, respectively. Furthermore, the prediction-correction procedure in Section IV-B is used to set the adaptive step size at each iteration.

For simplicity, we randomly chose the initial point for EIM. Note that this point may not be feasible for SINR constraint (4) in \mathcal{P}_1 . Also, since $\mathcal{P}_{1\text{fea}}$ is a non-convex optimization problem, EIM may not be guaranteed to converge or the terminating point may not be feasible as required for $\mathbf{v}^{(0)}$ for $\mathcal{P}_{1\text{SCA}}(\mathbf{v})$. Thus, EIM is served as a heuristic algorithm. If the point produced by EIM is infeasible, we may consider different initial points for EIM until a feasible is obtained. Our extensive simulation experiments show that EIM converges and provides a feasible initial point with a very high probability.

2) *SDR-based initialization method*: Similar to [2], we can apply SDR along with Gaussian randomization for $\mathcal{P}_{1\text{SCA}}^i(\mathbf{y})$ to obtain an approximate solution as a feasible initial point $\mathbf{y}^{(0)}$ for ESCA. Recall that \mathcal{P}_1 is converted from the original problem \mathcal{P}_o and is of relatively smaller size (K_{tot} variables and constraints). SDR can provide a point close to the local optimal point for small to moderate size of problems, resulting in fast convergence for ESCA. However, when K_{tot} becomes large, the computational complexity of SDR increases, and the quality of the initial point deteriorates.

V. ADMM-BASED SCA ALGORITHM

In this section, we propose another fast algorithm to solve each SCA subproblem $\mathcal{P}_{1\text{SCA}}(\mathbf{v})$ based on the ADMM technique [37]. Define the auxiliary variables $d_{jik} \triangleq \mathbf{a}_j^H \mathbf{f}_{jik}$, for $k \in \mathcal{K}_i, i, j \in \mathcal{G}$. Define $\mathbf{d} \triangleq [d_{11}^H, \dots, d_{GK_G}^H]^H \in \mathbb{C}^{GK_{\text{tot}}}$, with $\mathbf{d}_{ik} \triangleq [d_{1ik}, \dots, d_{Gik}]^T \in \mathbb{C}^G$. Then, the problem $\mathcal{P}_{1\text{SCA}}(\mathbf{v})$ can be equivalently expressed as

$$\mathcal{P}_{1\text{ADMM}}(\mathbf{v}) : \min_{\mathbf{a}, \mathbf{d}} \sum_{j=1}^G \|\mathbf{C}_j \mathbf{a}_j\|^2$$

$$\text{s.t. } d_{jik} = \mathbf{a}_j^H \mathbf{f}_{jik}, \quad k \in \mathcal{K}_i, i, j \in \mathcal{G} \quad (17)$$

$$\gamma_{ik} \sum_{j \neq i} |d_{jik}|^2 + |\mathbf{v}_i^H \mathbf{f}_{iik}|^2 + \gamma_{ik} \sigma^2 - 2\Re\{d_{iik} \mathbf{f}_{iik}^H \mathbf{v}_i\} \leq 0, \quad k \in \mathcal{K}_i, i \in \mathcal{G}. \quad (18)$$

Denote the feasible set for the inequality constraint (18) by \mathcal{F} . Define the indicator function for the set \mathcal{F} as

$$I_{\mathcal{F}}(\mathbf{d}) \triangleq \begin{cases} 0 & \text{if } \mathbf{d} \in \mathcal{F}, \\ \infty & \text{otherwise.} \end{cases}$$

Then, $\mathcal{P}_{1\text{ADMM}}(\mathbf{v})$ is equivalent to the following problem

$$\mathcal{P}'_{1\text{ADMM}}(\mathbf{v}) : \min_{\mathbf{a}, \mathbf{d}} \sum_{j=1}^G \|\mathbf{C}_j \mathbf{a}_j\|^2 + I_{\mathcal{F}}(\mathbf{d})$$

$$\text{s.t. } d_{jik} = \mathbf{a}_j^H \mathbf{f}_{jik}, \quad k \in \mathcal{K}_i, i, j \in \mathcal{G}. \quad (19)$$

By introducing the auxiliary vector \mathbf{d} in constraint (18), we construct the equality-constrained problem $\mathcal{P}'_{1\text{ADMM}}(\mathbf{v})$, where the objective function contains two separate terms for \mathbf{d} and \mathbf{a} only. This allows us to apply ADMM to decompose the problem into separate subproblems [37]. The augmented Lagrangian of $\mathcal{P}'_{1\text{ADMM}}(\mathbf{v})$ is given by

$$\mathcal{L}_{\rho}(\mathbf{d}, \mathbf{a}, \mathbf{q}) = \sum_{j=1}^G \|\mathbf{C}_j \mathbf{a}_j\|^2 + I_{\mathcal{F}}(\mathbf{d})$$

$$+ \frac{\rho}{2} \sum_{j=1}^G \sum_{i=1}^G \sum_{k=1}^{K_i} |d_{jik} - \mathbf{a}_j^H \mathbf{f}_{jik} + q_{jik}|^2 \quad (20)$$

where $\rho > 0$ is the penalty parameter, and $q_{jik} \in \mathbb{C}$ is the dual variable associated with constraint (19), and $\mathbf{q} \triangleq [q_{11}^H, \dots, q_{GK_G}^H]^H$, with $\mathbf{q}_{ik} \triangleq [q_{1ik}, \dots, q_{Gik}]^T$. We now decompose $\mathcal{L}_{\rho}(\mathbf{d}, \mathbf{a}, \mathbf{q})$ into two subproblems for \mathbf{d} and \mathbf{a} separately, and update $\{\mathbf{d}, \mathbf{a}, \mathbf{q}\}$ alternatively. Our proposed ADMM-based updating procedure for solving $\mathcal{P}'_{1\text{ADMM}}(\mathbf{v})$ is given as follows:

$$\mathbf{d}^{(n+1)} = \arg \min_{\mathbf{d}} \mathcal{L}_{\rho}(\mathbf{d}, \mathbf{a}^{(n)}, \mathbf{q}^{(n)}), \quad (21)$$

$$\mathbf{a}^{(n+1)} = \arg \min_{\mathbf{a}} \mathcal{L}_{\rho}(\mathbf{d}^{(n+1)}, \mathbf{a}, \mathbf{q}^{(n)}), \quad (22)$$

$$q_{jik}^{(n+1)} = q_{jik}^{(n)} + (d_{jik}^{(n+1)} - \mathbf{a}_j^{(n+1)H} \mathbf{f}_{jik}) \quad (23)$$

where n is the iteration index. Since $\mathcal{P}'_{1\text{ADMM}}(\mathbf{v})$ is convex, the above ADMM procedure is guaranteed to converge to the optimal solution of $\mathcal{P}_{1\text{ADMM}}(\mathbf{v})$ [37].

The two main updating steps in (21) and (22) involve solving two optimization problems. In the following, we derive the closed-form solutions for the two optimization problems in (21) and (22), which leads to fast computation at each iteration.

A. Closed-Form \mathbf{d} -Update

Given $\mathbf{a}^{(n)}$ and $\mathbf{q}^{(n)}$, from (20), the update of \mathbf{d} in (21) is equivalent to solving the following problem

$$\mathcal{P}_{\mathbf{d}}(\mathbf{v}) : \min_{\mathbf{d}} \sum_{j=1}^G \sum_{i=1}^G \sum_{k=1}^{K_i} |d_{jik} - \mathbf{a}_j^{(n)H} \mathbf{f}_{jik} + q_{jik}^{(n)}|^2 \quad \text{s.t. (18).}$$

Problem $\mathcal{P}_{\mathbf{d}}(\mathbf{v})$ can be decomposed into K_{tot} convex subproblems, one for each user k in group i given by

$$\mathcal{P}_{\text{dsub}}(\mathbf{v}) : \min_{\mathbf{d}_{ik}} \sum_{j=1}^G |d_{jik} - e_{1,jik}^{(n)}|^2$$

$$\text{s.t. } e_{2,ik} + \gamma_{ik} \sum_{j \neq i} |d_{jik}|^2 - 2\Re\{d_{iik} e_{3,ik}\} \leq 0 \quad (24)$$

where

$$e_{1,jik}^{(n)} \triangleq \mathbf{a}_j^{(n)H} \mathbf{f}_{jik} - q_{jik}^{(n)}, \quad e_{2,ik} \triangleq |\mathbf{v}_i^H \mathbf{f}_{iik}|^2 + \gamma_{ik} \sigma^2, \quad e_{3,ik} \triangleq \mathbf{f}_{iik}^H \mathbf{v}_i. \quad (25)$$

Problem $\mathcal{P}_{\text{dsub}}(\mathbf{v})$ is a convex QCQP-1 problem, whose solution may be derived in closed-form. In particular, a problem of similar structure has been considered in [21], where the closed-form solution is derived in [21, Appendix A]. We directly use this result and state the closed-form solution below. The optimal solution \mathbf{d}_{ik}^o for $\mathcal{P}_{\text{dsub}}(\mathbf{v})$ is given by

$$d_{jik}^o = \begin{cases} e_{1,ijk}^{(n)} + \nu_{ik}^o e_{3,ik}^* & \text{if } j = i, \\ \frac{e_{1,ijk}^{(n)}}{1 + \nu_{ik}^o \gamma_{ik}} & \text{otherwise.} \end{cases} \quad (26)$$

where $\nu_{ik}^o = 0$ if $e_{2,ik} + \gamma_{ik} \sum_{j \neq i} |e_{1,ijk}^{(n)}|^2 - 2\Re\{e_{3,ik} e_{1,ijk}^{(n)}\} \leq 0$; otherwise, ν_{ik}^o is the unique real positive root of the following cubic equation of ν_{ik} :

$$e_{2,ik} + \gamma_{ik} \frac{\sum_{j \neq i} |e_{1,ijk}^{(n)}|^2}{(1 + \nu_{ik} \gamma_{ik})^2} - 2\Re\{e_{3,ik} e_{1,ijk}^{(n)}\} - 2\nu_{ik} |e_{3,ik}|^2 = 0. \quad (27)$$

The roots of (27) are given by the cubic formula [21], and thus, ν_{ik}^o is obtained in closed-form. For the sake of completeness, the key steps leading to the above solution is provided in Appendix A.

B. Closed-Form \mathbf{a} -Update

Given $\mathbf{d}^{(n+1)}$ and $\mathbf{q}^{(n)}$, the update of \mathbf{a} in (22) is equivalent to solving the following problem

$$\mathcal{P}_a(\mathbf{v}): \min_{\mathbf{a}} \sum_{j=1}^G \left(\|\mathbf{C}_j \mathbf{a}_j\|^2 + \frac{\rho}{2} \sum_{i=1}^G \sum_{k=1}^{K_i} |d_{jik}^{(n+1)} - \mathbf{a}_j^H \mathbf{f}_{jik} + q_{jik}^{(n)}|^2 \right).$$

Problem $\mathcal{P}_a(\mathbf{v})$ can be decomposed into G subproblems, one for each group j expressed as

$$\mathcal{P}_{\text{asub}}(\mathbf{v}): \min_{\mathbf{a}_j} \|\mathbf{C}_j \mathbf{a}_j\|^2 + \frac{\rho}{2} \sum_{i=1}^G \sum_{k=1}^{K_i} |d_{jik}^{(n+1)} - \mathbf{a}_j^H \mathbf{f}_{jik} + q_{jik}^{(n)}|^2.$$

Problem $\mathcal{P}_{\text{asub}}(\mathbf{v})$ is an unconstrained convex optimization problem. Using the first-order optimality condition [18], we obtain the closed-form solution to $\mathcal{P}_{\text{asub}}(\mathbf{v})$ as

$$\mathbf{a}_j^{(n+1)} = \frac{\rho}{2} \left(\mathbf{C}_j^H \mathbf{C}_j + \frac{\rho}{2} \sum_{i=1}^G \sum_{k=1}^{K_i} \mathbf{f}_{jik} \mathbf{f}_{jik}^H \right)^{-1} \cdot \sum_{i=1}^G \sum_{k=1}^{K_i} \left(d_{jik}^{(n+1)} + q_{jik}^{(n)} \right)^* \mathbf{f}_{jik}. \quad (28)$$

We summarize the ASCA algorithm in Algorithm 2. The main computational complexity of ASCA lies in computing $\{e_{1,ijk}^{(n)}\}$ in (25) for $k \in \mathcal{K}_i, i, j \in \mathcal{G}$ and $\{\mathbf{a}_j^{(n+1)}\}$ in (28) for $j \in \mathcal{G}$ at each ADMM iteration. Note that computing $\mathbf{a}_j^{(n+1)}$ involves a matrix inversion with a complexity of $O(K_j^3)$. However, the matrix only depends on the channel vectors, and thus the matrix inversion only needs to be computed once at the beginning of ASCA. Thus for each ADMM iteration, only matrix-vector multiplications are involved. The related matrix-vector computation for $\{e_{1,ijk}^{(n)}\}$ and $\{\mathbf{a}_j^{(n+1)}\}$ requires a total of $8(\sum_{i=1}^G K_i)^2$ flops at each ADMM iteration. The number

Algorithm 2 ASCA Algorithm to Solve \mathcal{P}_1

- 1: **Initialization:** Set feasible initial point $\mathbf{v}^{(0)}$. Set $\rho; l = 0$.
 - 2: **repeat**
 - 3: // solve $\mathcal{P}_{1\text{ADMM}}(\mathbf{v}^{(l)})$
 - 4: **Initialization:** $\mathbf{a}^{(0)} = \mathbf{v}^{(l)}, \mathbf{d}^{(0)} = \mathbf{0}, \mathbf{q}^{(0)} = \mathbf{0}, n = 0$.
 - 5: **repeat**
 - 6: Compute $\mathbf{d}^{(n+1)}$ by (21) with $\mathbf{a}^{(n)}$ and $\mathbf{q}^{(n)}$.
 - 7: Compute $\mathbf{a}^{(n+1)}$ by (22) with $\mathbf{d}^{(n+1)}$ and $\mathbf{q}^{(n)}$.
 - 8: Compute $\mathbf{q}^{(n+1)}$ by (23) with $\mathbf{d}^{(n+1)}$ and $\mathbf{a}^{(n+1)}$.
 - 9: $n \leftarrow n + 1$.
 - 10: **until** convergence
 - 11: Set $\mathbf{v}^{(l+1)} = \mathbf{a}^{(n)}$. Set $l \leftarrow l + 1$.
 - 12: **until** convergence
-

of iterations for convergence depends on the problem size K_{tot} . From our experiments, it typically takes 50 ~ 150 iterations for $K_{\text{tot}} = 15 \sim 60$ users for ADMM to converge at each SCA iteration.

C. Initialization for ASCA

As discussed earlier in Section IV-C, a feasible initial point is required by SCA to solve \mathcal{P}_1 . Below we propose an ADMM-based initialization method (AIM).

Using the ADMM-based algorithm above, we propose AIM for ASCA. The feasible point is computed by solving the following feasibility problem

$$\mathcal{P}'_{1\text{fea}}: \text{Find } \{\mathbf{a}\} \quad \text{s.t. (4).}$$

Using the auxiliary variables $d_{jik} = \mathbf{a}_j^H \mathbf{f}_{jik}$, for $k \in \mathcal{K}_i, i, j \in \mathcal{G}$, defined at the beginning of Section V, $\mathcal{P}'_{1\text{fea}}$ is equivalently expressed as

$$\begin{aligned} \mathcal{P}'_{1\text{feaADMM}}: \text{Find } \{\mathbf{a}, \mathbf{d}\} \\ \text{s.t. } d_{jik} = \mathbf{a}_j^H \mathbf{f}_{jik}, \quad k \in \mathcal{K}_i, i, j \in \mathcal{G} \\ \frac{|d_{iik}|^2}{\sum_{j \neq i} |d_{jik}|^2 + \sigma^2} \geq \gamma_{ik}, \quad k \in \mathcal{K}_i, i \in \mathcal{G}. \end{aligned} \quad (29)$$

Denote the feasible set for constraint (29) by $\tilde{\mathcal{F}}$. The augmented Lagrangian of $\mathcal{P}'_{1\text{feaADMM}}$ is given by

$$\tilde{\mathcal{L}}_{\tilde{\rho}}(\mathbf{d}, \mathbf{a}, \tilde{\mathbf{q}}) = I_{\tilde{\mathcal{F}}}(\mathbf{d}) + \frac{\tilde{\rho}}{2} \sum_{j=1}^G \sum_{i=1}^G \sum_{k=1}^{K_i} |d_{jik} - \mathbf{a}_j^H \mathbf{f}_{jik} + \tilde{q}_{jik}|^2 \quad (30)$$

where indicator function I , penalty parameter $\tilde{\rho}$, dual variable \tilde{q}_{jik} are defined similarly as those in (20). Similar to the ADMM updating procedures in (21)–(23), based on (30), the AIM updating procedure for solving $\mathcal{P}'_{1\text{feaADMM}}$ is given as follows: At iteration $n + 1$,

$$\mathbf{d}^{(n+1)} = \arg \min_{\mathbf{d} \in \tilde{\mathcal{F}}} \sum_{j=1}^G \sum_{i=1}^G \sum_{k=1}^{K_i} |d_{jik} - \mathbf{a}_j^{(n)H} \mathbf{f}_{jik} + \tilde{q}_{jik}^{(n)}|^2, \quad (31)$$

$$\mathbf{a}^{(n+1)} = \arg \min_{\mathbf{a}} \sum_{j=1}^G \sum_{i=1}^G \sum_{k=1}^{K_i} |d_{jik}^{(n+1)} - \mathbf{a}_j^H \mathbf{f}_{jik} + \tilde{q}_{jik}^{(n)}|^2, \quad (32)$$

$$\tilde{q}_{jik}^{(n+1)} = \tilde{q}_{jik}^{(n)} + (d_{jik}^{(n+1)} - \mathbf{a}_j^{(n+1)H} \mathbf{f}_{jik}). \quad (33)$$

The updating steps in (31) and (32) can be derived in closed-form, which are provided in Appendix B.

The initial point for AIM is randomly chosen, which may not be feasible for SINR constraint (29) in $\mathcal{P}'_{\text{1feaADMM}}$. However, if AIM converges, the terminating point will satisfy SINR constraint (29), and the produced point \mathbf{a} for $\mathbf{v}^{(0)}$ is feasible to $\mathcal{P}_{\text{1SCA}}(\mathbf{v})$. Note that since $\mathcal{P}'_{\text{1fea}}$ is a non-convex optimization problem, the ADMM procedure for AIM described above may not be guaranteed to converge. Thus, AIM is served as a heuristic algorithm. Our extensive simulation studies show that AIM converges to a feasible point with a very high probability.

Besides AIM, We can also use the SDR-based initialization method discussed in Section IV-C for initialization of ASCA, where a feasible initial points $\mathbf{v}^{(0)}$ for ASCA is obtained by applying SDR along with Gaussian randomization to solve \mathcal{P}_1 .

Remark 2. We point out that the initialization methods EIM and AIM proposed in Sections IV-C and V-C can be used for initialization in both Algorithms 1 and 2, or any SCA-based algorithm.

VI. SCALING SCHEME FOR THE MMF PROBLEM

In this section, with the proposed ESCA and ASCA for the QoS problem, we propose an efficient scheme to obtain a solution to the MMF problem \mathcal{S}_o .

We transform the original MMF problem \mathcal{S}_o into the following equivalent problem

$$\mathcal{S}'_o(\boldsymbol{\gamma}, P) : \max_{\mathbf{w}, t} t \quad \text{s.t.} \quad \text{SINR}_{ik} \geq t\gamma_{ik}, \quad k \in \mathcal{K}_i, i \in \mathcal{G} \\ \sum_{i=1}^G \|\mathbf{w}_i\|^2 \leq P$$

where vector $\boldsymbol{\gamma}$ contains all SINR targets $\{\gamma_{ik}\}$ of all users in all groups. Furthermore, we parameterize the QoS problem \mathcal{P}_o as $\mathcal{P}_o(\boldsymbol{\gamma})$. It has been shown that $\mathcal{S}'_o(\boldsymbol{\gamma}, P)$ and $\mathcal{P}_o(t\boldsymbol{\gamma})$ are the inverse problems to each other [5]. Specifically, denote the maximum objective value of $\mathcal{S}'_o(\boldsymbol{\gamma}, P)$ by $t^o = \mathcal{S}'_o(\boldsymbol{\gamma}, P)$. Let the minimum power objective value of $\mathcal{P}_o(\boldsymbol{\gamma}')$ be $P = \mathcal{P}_o(\boldsymbol{\gamma}')$ for some $\boldsymbol{\gamma}'$. Then, we have the following inverse relation:

$$t^o = \mathcal{S}'_o(\boldsymbol{\gamma}, \mathcal{P}_o(t^o\boldsymbol{\gamma})), \quad P = \mathcal{P}_o(\mathcal{S}'_o(\boldsymbol{\gamma}, P)\boldsymbol{\gamma}). \quad (34)$$

Based on this relation, in the literature, the MMF problem $\mathcal{S}'_o(\boldsymbol{\gamma}, P)$ is typically solved via iteratively solving the QoS problem $\mathcal{P}_o(t\boldsymbol{\gamma})$ along with a bi-section search over t until the transmit power objective in $\mathcal{P}_o(t\boldsymbol{\gamma})$ is equal to P [2], [5], [6], [17], [21]. However, this approach is computationally expensive. As mentioned at the end of Section III-B, existing works use either SDR or SCA to compute a solution to $\mathcal{P}_o(t\boldsymbol{\gamma})$, where the second-order IPM method is used to solve either relaxed or convexified approximate problem. As a result, iteratively solving $\mathcal{P}_o(t\boldsymbol{\gamma})$ incurs high computational complexity not suitable for large-scale problems. Using the optimal beamforming structure \mathbf{w}_i^o in (3) can significantly reduce the required computation in the above approach, where $\mathcal{P}_o(t\boldsymbol{\gamma})$ can be converted to a much smaller weight optimization problem as in \mathcal{P}_1 . Nonetheless, resorting to the additional layer of iterations to solve the QoS problem is still computationally costly for the MMF problem as compared with the QoS problem itself, especially for large-scale problems [2].

To avoid the additional iterative procedure, we develop a closed-form scaling scheme for finding a solution to \mathcal{S}_o directly. Specifically, we first obtain the solution to $\mathcal{P}_o(\boldsymbol{\gamma})$ by solving the smaller weight optimization problem \mathcal{P}_1 using either ESCA

Algorithm 3 The Closed-Form Scaling Scheme for $\mathcal{S}_o(\boldsymbol{\gamma}, P)$

- 1: Solve $\mathcal{P}_o(\boldsymbol{\gamma})$ and attain solution $\mathbf{w}^o(\boldsymbol{\gamma})$.
 - 2: Compute $P^o(\boldsymbol{\gamma}) = \sum_{i=1}^G \|\mathbf{w}_i^o(\boldsymbol{\gamma})\|^2$.
 - 3: Compute $\mathbf{w}^s(\boldsymbol{\gamma}, P) = \sqrt{\frac{P}{P^o(\boldsymbol{\gamma})}} \mathbf{w}^o(\boldsymbol{\gamma})$ as the solution to $\mathcal{S}_o(\boldsymbol{\gamma}, P)$.
-

or ASCA proposed in Sections IV and V. Then, we scale this solution to $\mathcal{P}_o(\boldsymbol{\gamma})$ to obtain a solution to $\mathcal{S}'_o(\boldsymbol{\gamma}, P)$, such that the transmit power budget P is met. Parameterize \mathcal{S}_o as $\mathcal{S}_o(\boldsymbol{\gamma}, P)$. This proposed scaling scheme is summarized in Algorithm 3. We show below that this scaling scheme provides a feasible solution to $\mathcal{S}_o(\boldsymbol{\gamma}, P)$, and we also bound its performance.

Proposition 1. Let $\mathbf{w}^o(\boldsymbol{\gamma})$ be a feasible beamforming solution to $\mathcal{P}_o(\boldsymbol{\gamma})$ produced by a given algorithm, with the achieved objective value denoted by $P^o(\boldsymbol{\gamma})$. Define $I_{ik}^o(\boldsymbol{\gamma}) \triangleq \sum_{j \neq i} |\mathbf{h}_{ik}^H \mathbf{w}_j^o(\boldsymbol{\gamma})|^2$. Then, the scaled beamforming vector $\mathbf{w}^s(\boldsymbol{\gamma}, P) \triangleq \sqrt{\frac{P}{P^o(\boldsymbol{\gamma})}} \mathbf{w}^o(\boldsymbol{\gamma})$ is a feasible solution to $\mathcal{S}_o(\boldsymbol{\gamma}, P)$; the corresponding achieved objective value, denoted by $t^s(\boldsymbol{\gamma}, P)$, satisfies

$$\frac{P}{P^o(\boldsymbol{\gamma})} \min_{i,k} \frac{I_{ik}^o(\boldsymbol{\gamma}) + \sigma^2}{\frac{P}{P^o(\boldsymbol{\gamma})} I_{ik}^o(\boldsymbol{\gamma}) + \sigma^2} \leq t^s(\boldsymbol{\gamma}, P) \\ \leq \frac{P}{P^o(\boldsymbol{\gamma})} \max_{i,k} \frac{I_{ik}^o(\boldsymbol{\gamma}) + \sigma^2}{\frac{P}{P^o(\boldsymbol{\gamma})} I_{ik}^o(\boldsymbol{\gamma}) + \sigma^2} \quad (35)$$

where $P^o(\boldsymbol{\gamma})$ denotes the optimal objective value of $\mathcal{P}_o(\boldsymbol{\gamma})$.

Proof: See Appendix C. ■

Note that the tightness of the lower and upper bounds for $t^s(\boldsymbol{\gamma}, P)$ in (35) depends on transmit power $P^o(\boldsymbol{\gamma})$, which is obtained by a given algorithm for $\mathcal{P}_o(\boldsymbol{\gamma})$ with solution $\mathbf{w}^o(\boldsymbol{\gamma})$. If the power budget P for the MMF problem $\mathcal{S}_o(\boldsymbol{\gamma}, P)$ is more than the optimal power value for $\mathcal{P}_o(\boldsymbol{\gamma})$, i.e., $P \geq P^o(\boldsymbol{\gamma})$, and the algorithm provides $P^o(\boldsymbol{\gamma}) = P$, then $\mathbf{w}^s(\boldsymbol{\gamma}, P) = \mathbf{w}^o(\boldsymbol{\gamma})$, and the bounds in (35) in this case are simplified to $1 \leq t^s(\boldsymbol{\gamma}, P) \leq \frac{P}{P^o(\boldsymbol{\gamma})}$. Note that, often for the given algorithm, the solution $\mathbf{w}^o(\boldsymbol{\gamma})$ results in at least one SINR constraint being attained with equality, i.e., $\text{SINR}_{ik} = \gamma_{ik}$, for some i, k , then we have $t^s(\boldsymbol{\gamma}, P) = 1$. In a special case when $P^o(\boldsymbol{\gamma}) = P = P^o(\boldsymbol{\gamma})$, we have $t^s(\boldsymbol{\gamma}, P) = 1$, and also both the upper and lower bounds become 1. In this case, since $P = P^o(\boldsymbol{\gamma})$, from the inverse relation in (34), we have $t^o = 1$. Thus, $t^s(\boldsymbol{\gamma}, P) = t^o = 1$, and the bounds in (35) are tight.

Comparing Algorithm 3 with the iterative bi-section search method using (34), we see that our proposed closed-form scaling scheme avoids iteratively solving $\mathcal{P}_2(t\boldsymbol{\gamma})$ along with a bi-section search over t , and thereby, enjoys a significant reduction of computational complexity. Moreover, we can directly apply the fast algorithm ESCA proposed in Section IV or ASCA proposed in Section V along with the optimal structure in (3) to provide a solution to $\mathcal{P}_o(\boldsymbol{\gamma})$ with this scaling scheme. This approach leads to two fast first-order algorithms for solving $\mathcal{S}_o(\boldsymbol{\gamma}, P)$ in large-scale systems.

Remark 3. We point out that our scaling scheme for the multi-group multicast beamforming MMF problem is different from a similar scaling scheme proposed for the MMF problem in a single-group scenario in [22]. Specifically, the scheme in

[22] first applies ZF beamforming for each group to eliminate inter-group interference. Once the interference is removed, for the equivalent single-group multicast beamforming problem, [22] scales the beamforming solution of the single-group QoS problem to obtain a feasible solution to the MMF problem. In our scheme, we directly handle the original multi-group MMF problem containing inter-group interference. Our scheme scales the solution of the multi-group QoS problem $\mathcal{P}_o(\gamma)$ to solve the original MMF problem $\mathcal{S}_o(\gamma, P)$. Note that the scheme in [22] has the lower and upper bounds for the objective value t (similar to t in $\mathcal{S}'_o(\gamma, P)$) as $\left[\frac{P}{P^o(\gamma)}, \frac{P}{P^o(\gamma)}\right]$ with no interference present. In contrast, for our scheme, the lower and upper bounds in (35) contain additional terms w.r.t. $I_{ik}^o(\gamma)$. Note that $I_{ik}^o(\gamma)$ represents the inter-group interference to user k in group i by solution $\mathbf{w}^o(\gamma)$. Following this, both terms $I_{ik}^o(\gamma) + \sigma^2$ and $\frac{P}{P^o(\gamma)}I_{ik}^o(\gamma) + \sigma^2$ in (35) are the interference plus noise term for user k in group i , where the latter is based on the scaled beamforming solution $\mathbf{w}^s(\gamma, P)$. These additional terms in the lower and upper bounds in (35) represent the minimum and maximum inter-group interference ratios, respectively. In the special case of single group $G = 1$, the bounds in (35) reduces to $\left[\frac{P}{P^o(\gamma)}, \frac{P}{P^o(\gamma)}\right]$ in [22]. Thus, the bounds in (35) can be viewed as a generalization of the bounds in [22] from single-group to multi-group settings with inter-group interference.

VII. SIMULATION RESULTS

We consider a default setup for downlink multi-group multi-cast beamforming, where $G = 3$ groups, $K_i = K$ users/group, $\forall i \in \mathcal{G}$, and the same SINR target for each user $\gamma_{ik} = \gamma$, for all k, i . The user channels are generated independently with an identical distribution as $\mathbf{h}_{ik} \sim \mathcal{CN}(\mathbf{0}, \mathbf{I})$. The performance plots are obtained by averaging the results over 100 channel realizations per user.

For QoS problem \mathcal{P}_o , we consider the proposed two fast algorithms: ESCA in Algorithm 1 and ASCA in Algorithm 2. For ESCA, we set the step size $\alpha = 0.1$ and the constant $c = 0.8$. For ASCA, we set the penalty parameter $\rho = 0.2$ ¹. We consider different initialization methods discussed in Sections IV-C and V-C for ESCA and ASCA, respectively. Therefore, we refer to our algorithms as follows: 1) EIM-ESCA: ESCA with EIM initialization; 2) SDR-ESCA: ESCA with SDR initialization; 3) AIM-ASCA: ASCA with AIM initialization; 4) SDR-ASCA: ASCA with SDR initialization. Note that each algorithm solves the weight optimization problem \mathcal{P}_1 using the optimal beamforming structure in (3)². Besides the above four algorithms for solving \mathcal{P}_1 , we also consider the following methods for comparison:

- Lower Bound for \mathcal{P}_o : Obtained by solving the relaxed version of \mathcal{P}_o via SDR.
- SDR-CSCA: Solve \mathcal{P}_1 via SCA using $\mathcal{P}_{1\text{SCA}}(\mathbf{v})$, where each $\mathcal{P}_{1\text{SCA}}(\mathbf{v})$ is solved by the standard convex solver CVX, which uses IPM [2]. The SDR method is used to generate an initial point.

¹We have studied different values of ρ and found $\rho = 0.2$ generally provides overall good performance and convergence speed for ASCA.

²Note that in (3), the exact expression of $\mathbf{R}(\lambda^o)$ is used and its computation is discussed below (3). One may utilize the asymptotic expression of $\mathbf{R}(\lambda^o)$ obtained in [2] to simplify the computation of $\mathbf{R}(\lambda^o)$. Since the fixed-point iterative method [2] for computing $\mathbf{R}(\lambda^o)$ is computationally inexpensive, using the asymptotic expression of $\mathbf{R}(\lambda^o)$ only brings a minor reduction of computation cost and thus is not considered in the simulation.

For MMF problem \mathcal{S}_o , we consider ESCA and ASCA with the proposed scaling scheme in Algorithm 3. They are denoted as ESCA-Scaling and ASCA-Scaling, respectively. For comparison, we also consider the following methods:

- Upper Bound for \mathcal{S}_o : Obtained by solving the relaxed version of \mathcal{P}_o using SDR along with the bi-section search over t .
- ESCA-Bisection: Solve \mathcal{S}_o via iteratively solving \mathcal{P}_o along with bi-section search over t . For solving \mathcal{P}_o , SDR-ESCA is used, where the optimal beamforming structure in (3) with the asymptotic expression of $\mathbf{R}(\lambda^o)$ obtained in [2] is applied.
- ASCA-Bisection: Similar to ESCA-Bisection, except that SDR-ASCA is used to solve \mathcal{P}_o .
- CSCA-Bisection [2]: Similar to ESCA-Bisection, except that SDR-CSCA is used to solve \mathcal{P}_o .
- SDR-Bisection [2]: Solve \mathcal{S}_o via iteratively solving \mathcal{P}_o along with bi-section search over t . For solving \mathcal{P}_o , SDR along with the Gaussian randomization method is used, where the optimal beamforming structure in (3) with the asymptotic expression of $\mathbf{R}(\lambda^o)$ is applied.

A. Convergence Analysis

In this subsection, we study the convergence behavior of the two proposed fast algorithms (ESCA and ASCA) for the QoS problem \mathcal{P}_o . Note that each algorithm consists of two layers of iterations: Outer-layer SCA and the inner-layer iterative algorithm to solve each $\mathcal{P}_{1\text{SCA}}(\mathbf{v})$. Let $P_t = \sum_{i=1}^G \|\mathbf{w}_i\|^2$ denote the total transmit power. Fig. 1 shows the trajectory of normalized transmit power P_t/σ^2 over the inner-layer iterations at the first outer-layer SCA iteration. We set $N = 500$ and $K = 10$. We observe that SDR-ESCA and SDR-ASCA converge faster and result in lower P_t/σ^2 than EIM-ESCA and AIM-ASCA. This shows that the SDR initialization method provides a better initial point than the other initialization methods. Between SDR-ESCA and SDR-ASCA, we observe a similar convergence rate. Comparing EIM-ESCA and AIM-ASCA, we see that AIM-ASCA converges faster than EIM-ESCA. Next, we consider the convergence behavior of the relative difference of the optimization variable for each algorithm. Specifically, we consider the normalized difference $\frac{\|\mathbf{x}^{(n+1)} - \mathbf{x}^{(n)}\|}{\|\mathbf{x}^{(n+1)}\|}$ in two consecutive inner-layer iterations of ESCA in Algorithm 1, and similarly, $\frac{\|\mathbf{a}^{(n+1)} - \mathbf{a}^{(n)}\|}{\|\mathbf{a}^{(n+1)}\|}$ for ASCA in Algorithm 2. Fig. 2 shows these relative differences for different algorithms at the first outer-layer SCA iteration for $N = 500$ and $K = 10$. Again, we observe that the SDR initialization method results in a faster convergence than the other initialization methods. Both SDR-ESCA and SDR-ASCA reach a relative difference of 10^{-3} within 50 iterations, with SDR-ASCA converging slightly faster than SDR-ESCA. Comparing EIM-ESCA and AIM-ASCA, we see that AIM-ASCA provides a faster convergence than EIM-ESCA, reaching a relative difference of 10^{-3} within 50 iterations.

We now study the convergence behavior of different algorithms over the outer-layer SCA iterations. Fig. 3 shows the convergence behavior of our proposed algorithms at the outer-layer SCA iterations, for $N = 500$ and $K = 10$. We set the inner-layer convergence threshold for the proposed algorithms such that they converge to nearly the same value. For EIM-ESCA and SDR-ESCA, we set the inner-layer convergence

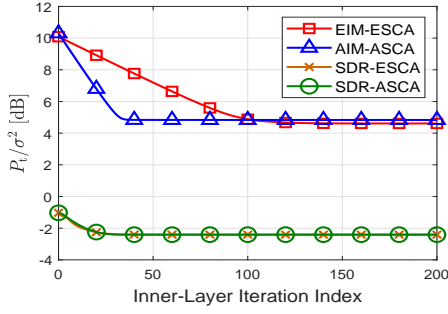


Fig. 1. Convergence behavior for \mathcal{P}_o : Normalized power objective P_t/σ^2 over the inner-layer iterations at the first outer-layer SCA iteration. ($N = 500$, $K = 10$).

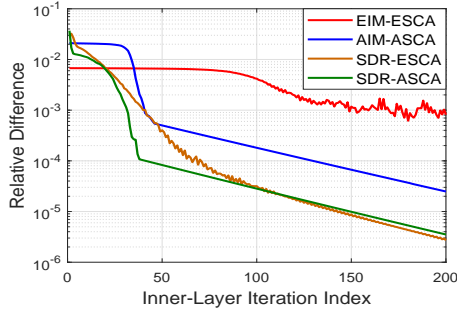


Fig. 2. Convergence behavior for \mathcal{P}_o : Relative difference over the inner-layer iterations at the first outer-layer SCA iteration. ($N = 500$, $K = 10$).

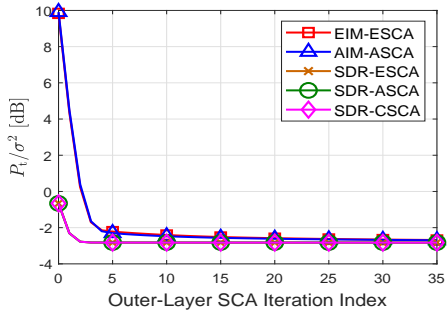


Fig. 3. Convergence behavior for \mathcal{P}_o : Normalized power objective P_t/σ^2 over the outer-layer SCA iterations. ($N = 500$, $K = 10$).

threshold to be $\frac{\|\mathbf{x}^{(n+1)} - \mathbf{x}^{(n)}\|}{\|\mathbf{x}^{(n+1)}\|} \leq 10^{-3}$. Note that although Fig. 1 shows that at the first outer-layer SCA iteration, EIM-ESCA converges to a higher value of P_t/σ^2 than that of SDR-ESCA over the inner-layer iterations, Fig. 3 shows that EIM-ESCA eventually converges to nearly the same value of P_t/σ^2 as that of SDR-ESCA over the outer-layer SCA iterations. For ASCA, we set the inner-layer convergence threshold $\frac{\|\mathbf{a}^{(n+1)} - \mathbf{a}^{(n)}\|}{\|\mathbf{a}^{(n+1)}\|} \leq 10^{-3}$ for SDR-ASCA and $\frac{\|\mathbf{a}^{(n+1)} - \mathbf{a}^{(n)}\|}{\|\mathbf{a}^{(n+1)}\|} \leq 0.2 \times 10^{-3}$ for AIM-ASCA. Our experiments show that a tighter inner-layer threshold for AIM-ASCA than that of SDR-ASCA is needed to converge to the same value of P_t/σ^2 as the rest of algorithms at the outer-layer iterations. As we see in Fig. 3, all algorithms converge to the same value of the normalized transmit power P_t/σ^2 within 35 SCA iterations. Again, comparing different initialization methods, we see that the SDR method provides a faster convergence for both ESCA and ASCA than EIM and AIM methods, where only less than 5 SCA iterations are required to reach convergence.

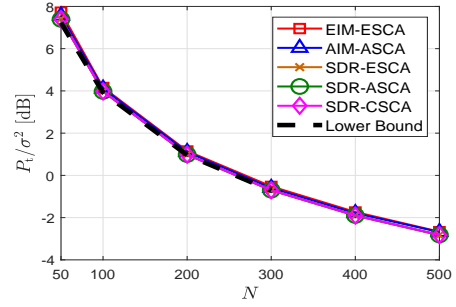


Fig. 4. QoS: Normalized transmit power P_t/σ^2 vs. N ($G = 3$, $K = 10$).

TABLE I
QoS: AVERAGE COMPUTATION TIME OVER N (SEC.) ($G = 3$, $K = 10$)

N	100	200	300	400	500
EIM-ESCA	2.694	3.032	2.708	2.589	2.711
AIM-ASCA	1.150	2.415	3.195	4.092	4.339
SDR-ESCA	0.327	0.237	0.233	0.224	0.243
SDR-ASCA	0.076	0.051	0.061	0.071	0.088
SDR-CSCA [2]	7.179	6.126	6.400	5.963	6.500
EIM (Init. method)	0.037	0.044	0.045	0.050	0.057
AIM (Init. method)	0.0068	0.0058	0.0059	0.0063	0.0073
SDR (Init. method)	1.050	1.038	1.104	1.103	1.137

B. Performance Comparison for the QoS Problem

We now compare the performance of different algorithms for the QoS problem. We set SINR target $\gamma = 10$ dB. Also, for all algorithms in comparison, we set the convergence threshold for the outer-layer SCA iterations as $\frac{\|\mathbf{v}^{(l+1)} - \mathbf{v}^{(l)}\|}{\|\mathbf{v}^{(l+1)}\|} \leq 10^{-3}$. Fig. 4 shows the normalized transmit power P_t/σ^2 vs. N by different algorithms, for $G = 3$ and $K = 10$. We see that our proposed algorithms have a similar performance to that of SDR-CSCA in [2], and all algorithms nearly attain the lower bound for \mathcal{P}_o . This demonstrates that our proposed fast algorithms achieve a near-optimal performance. The computational advantages of ESCA and ASCA are shown in Table I, where we list the average computation time by each algorithm used for the plots in Fig. 4. The first five rows show the computation times of different algorithms, excluding the initialization. We observe that, by using the optimal structure in (3), the computation times of all algorithms remain roughly unchanged as N increases. Under the same SDR initialization method, the computation times of SDR-ESCA and SDR-ASCA are only about 4% and 1% of that of SDR-CSCA, respectively, and SDR-ASCA has a smaller computation time than SDR-ESCA. The computation times of EIM-ESCA and AIM-ASCA are both about 40% of that of SDR-CSCA. The computation time of AIM-ASCA increases with N more noticeably than other algorithms. As a result, AIM-ASCA is initially faster than EIM-ESCA for $N < 300$, but becomes slower than EIM-ESCA for $N \geq 300$. The reason is due to the initialization as will be explained below. The last three rows in Table I show the computation times of different initialization methods. We see that the EIM is a fast initialization method, with its computation time about 4% of that of SDR. The AIM is the fastest one among all three initialization methods, with its computation time about 15% and 0.5% of that of EIM and SDR, respectively. However, the computation time of AIM-ASCA increases more obviously as N increases. This indicates that the quality of AIM initialization deteriorates as N increases,

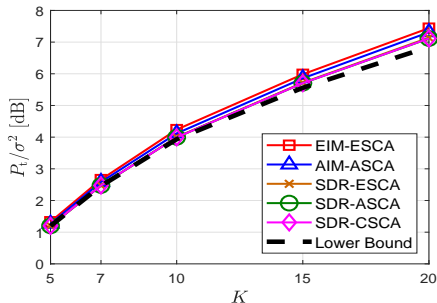
Fig. 5. QoS: Normalized transmit power P_t/σ^2 vs. K ($G = 3$, $N = 100$).

TABLE II

QoS: AVERAGE COMPUTATION TIME OVER K (SEC.) ($G = 3$, $N = 100$)

K	5	7	10	15	20
EIM-ESCA	1.098	1.689	2.737	5.498	8.685
AIM-ASCA	0.519	0.725	1.234	2.043	3.146
SDR-ESCA	0.056	0.112	0.373	0.856	1.666
SDR-ASCA	0.012	0.024	0.087	0.216	0.433
SDR-CSCA [2]	1.747	3.502	7.592	13.79	21.52
EIM (Init. method)	0.019	0.025	0.038	0.063	0.090
AIM (Init. method)	0.0048	0.0055	0.0067	0.012	0.018
SDR (Init. method)	0.545	0.727	1.094	1.852	3.489

unlike other initialization methods, leading to more iterations for convergence and a longer computation time.

Fig. 5 shows P_t/σ^2 vs. K by different algorithms, for $G = 3$ and $N = 100$. Again, the performance of SDR-ESCA and SDR-ASCA are nearly identical to that of SDR-CSCA and nearly attain the lower bound. The performance gaps of EIM-ESCA and AIM-ASCA to the lower bound are more noticeable as K becomes large, although they are still within 0.6 dB. Similar to Table I, the corresponding average computation times of these algorithms are shown in Table II. We see that both ESCA and ASCA are considerably faster than CSCA. In particular, their computation times only mildly increase with K , as compared with CSCA. For the initialization methods, EIM and AIM are faster than SDR and remain almost unchanged over K , while the complexity of SDR increases more noticeably over K . Overall, in terms of the total computation time, for $K < 20$, SDR-ESCA is faster than EIM-ESCA, and SDR-ASCA is comparable to AIM-ASCA; among all algorithms, SDR-ASCA provides the best performance with the fastest computation time. However, as both N and K become large (e.g., $N \geq 400$, $K \geq 20$), SDR-based initialization becomes computationally expensive, and the trends in Tables I and II indicate that EIM-ESCA provides the fastest computation time than the other algorithms.

C. Performance Comparison for the MMF Problem

We now present the performance of our proposed Algorithm 3 for the MMF problem \mathcal{S}_o . We set the maximum transmit power budget against noise variance as $P/\sigma^2 = 10$ dB. Fig. 6 plots the average minimum SINR vs. N , and Table III shows the corresponding computation time by these algorithms, for $G = 3$ and $K = 10$. Both ESCA-Bisection and ASCA-Bisection provide near-identical performance to that of CSCA-Bisection, and they are nearly optimal as compared with the upper bound, but with much lower computation times. The proposed simple ESCA-Scaling and ASCA-Scaling algorithms

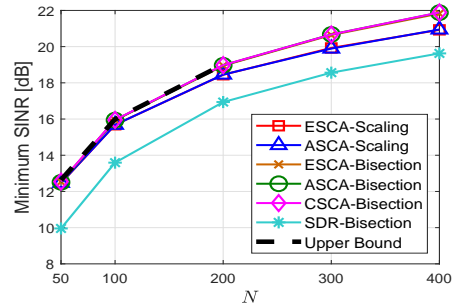
Fig. 6. MMF: Minimum SINR vs. N ($G = 3$, $K = 10$).

TABLE III

MMF: AVERAGE COMPUTATION TIME OVER N (SEC.) ($G = 3$, $K = 10$)

N	50	100	200	300	400
ESCA-Scaling	0.482	0.327	0.237	0.233	0.224
ASCA-Scaling	0.099	0.076	0.051	0.061	0.071
ESCA-Bisection	16.43	21.11	33.02	46.18	44.63
ASCA-Bisection	12.35	12.11	13.06	14.09	17.94
CSCA-Bisection [2]	99.04	87.33	81.62	84.10	99.86
SDR-Bisection [2]	11.19	15.46	19.85	15.82	22.12

for the MMF problem nearly attain the upper bound for $N \leq 100$. Their performance gap to the upper bound increases as N increases, indicating the accuracy of the scaling degrades as N becomes large. At $N = 400$, the gap is about 1 dB. Nonetheless, the ESCA-Scaling and ASCA-Scaling are several orders of magnitude faster than ESCA-Bisection and ASCA-Bisection. SDR-Bisection has worse performance than all the rest algorithms. This is because, for the QoS problem \mathcal{P}_1 at each bi-section iteration, the SDR approximation deteriorates when the number of constraints (GK) for \mathcal{P}_1 is large. Finally, Fig. 7 shows the average minimum SINR vs. K by different algorithms, for $G = 3$ and $N = 100$, with the corresponding computation time shown in Table IV. Except for the SDR-Bisection, all the proposed algorithms nearly attain the upper bound and thus are nearly optimal. In particular, ESCA-Scaling and ASCA-Scaling maintain their near-optimal performance as K increases. The computational advantage of ESCA-Scaling and ASCA-Scaling is clearly seen in Table IV, where both algorithms are substantially faster in computing a solution than the other algorithms.

VIII. CONCLUSION

In this work, exploiting the optimal multicast beamforming structure, we proposed two fast computational algorithms, ESCA and ASCA, for multi-group multicast beamforming design. For the QoS problem solved by the SCA method, these two algorithms provide efficient computational methods for solving the convex subproblems of SCA. At each SCA iteration, ESCA implements a dual saddle point reformulation along with the extragradient method to solve the convex subproblem; ASCA constructs an ADMM procedure in a form that decomposes the convex subproblem into multiple smaller subproblems for parallel computing with closed-form updates. To provide effective initial feasible points for SCA to facilitate fast convergence, we proposed three initialization methods based on the extragradient method, ADMM, and SDR. For the MMF problem, we further proposed a simple closed-form scaling approach based on the solution to the QoS problem, avoiding the high computational

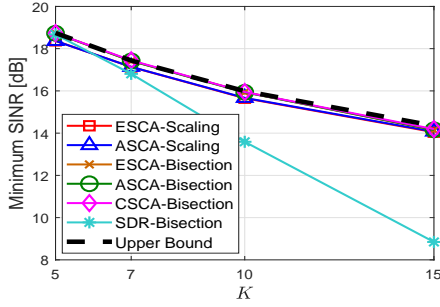


Fig. 7. MMF: Minimum SINR vs. K ($G = 3$, $N = 100$).

TABLE IV
MMF: AVERAGE COMPUTATION TIME OVER K (SEC.) ($G = 3$, $N = 100$)

K	5	7	10	15
ESCA-Scaling	0.056	0.112	0.373	0.856
ASCA-Scaling	0.012	0.024	0.087	0.216
ESCA-Bisection	7.297	12.62	21.26	39.59
ASCA-Bisection	6.192	8.628	12.13	25.18
CSCA-Bisection [2]	24.91	48.47	88.40	178.5
SDR-Bisection [2]	6.300	10.10	15.53	25.75

complexity involved in iteratively solving the QoS problems, while offering bounded performance guarantee. Our simulation studies showed that the proposed ESCA and ASCA provide near-optimal performance with substantially lower computational complexity than the state-of-the-art algorithms for large-scale systems.

APPENDIX A DERIVATION OF CLOSED-FORM \mathbf{d}_{ik}^o

The Lagrangian of $\mathcal{P}_{\text{dsub}}(\mathbf{v})$ is given by

$$\begin{aligned} \mathcal{L}(\mathbf{d}_{ik}, \nu_{ik}) &= \sum_{j=1}^G |d_{jik} - e_{1,jik}^{(n)}|^2 + \nu_{ik} e_{2,ik} \\ &\quad + \nu_{ik} \gamma_{ik} \sum_{j \neq i} |d_{jik}|^2 - 2\nu_{ik} \Re\{e_{3,ik} e_{1,ik}^{(n)}\} \end{aligned}$$

where $\nu_{ik} \geq 0$ is the dual variable associated with constraint (24). Since $\mathcal{P}_{\text{dsub}}(\mathbf{v})$ is convex, the optimal \mathbf{d}_{ik}^o and ν_{ik}^o satisfy the KKT conditions [18]. Setting the gradient $\nabla_{\mathbf{d}_{ik}} \mathcal{L}(\mathbf{d}_{ik}, \nu_{ik}^o) = 0$, we obtain \mathbf{d}_{ik}^o in (26). Substituting the expression of d_{jik}^o in (26) into the constraint of $\mathcal{P}_{\text{dsub}}(\mathbf{v})$ yields

$$\begin{aligned} f(\nu_{ik}^o) &\triangleq e_{2,ik} + \gamma_{ik} \sum_{j \neq i} \frac{|e_{1,jik}^{(n)}|^2}{(1 + \nu_{ik}^o \gamma_{ik})^2} - 2\Re\{e_{3,ik} e_{1,ik}^{(n)}\} \\ &\quad - 2\nu_{ik}^o |e_{3,ik}|^2 \leq 0. \end{aligned}$$

It is shown in [21, Appendix A] that the function $f(\nu_{ik}^o)$ is strictly decreasing w.r.t. $\nu_{ik}^o \geq 0$. Under the complementary slackness condition in the KKT conditions, we have $\nu_{ik}^o f(\nu_{ik}^o) = 0$. If $f(0) \leq 0$, then $f(\nu_{ik}^o) < 0$ for any $\nu_{ik}^o \geq 0$, and we have $\nu_{ik}^o = 0$; otherwise, $\nu_{ik}^o = 0$ is an infeasible dual solution for $\mathcal{P}_{\text{dsub}}(\mathbf{v})$, and thus, $f(\nu_{ik}^o) = 0$, and ν_{ik}^o is the unique real positive root of the cubic equation (27), whose roots can be obtained by the cubic formula [21].

APPENDIX B CLOSED-FORM UPDATING STEPS FOR AIM

1) *Closed-Form d-update in (31)*: Similar to that in Section V-A, given $\mathbf{a}^{(n)}$ and $\tilde{\mathbf{q}}^{(n)}$, the optimization problem in (31) can be decomposed into K_{tot} subproblems, one for each user k in group i given by

$$\begin{aligned} \mathcal{P}'_{\text{dsub}} : \min_{\mathbf{d}_{ik}} & \sum_{j=1}^G |d_{jik} - \tilde{e}_{1,jik}^{(n)}|^2 \\ \text{s.t.} & \gamma_{ik} \sum_{j \neq i} |d_{jik}|^2 + \gamma_{ik} \sigma^2 - |d_{iik}|^2 \leq 0. \end{aligned} \quad (36)$$

where $\tilde{e}_{1,jik}^{(n)} \triangleq \mathbf{a}_j^{(n)H} \mathbf{f}_{jik} - \tilde{q}_{jik}^{(n)}$, for $k \in \mathcal{K}_i$, $i, j \in \mathcal{G}$. Problem $\mathcal{P}'_{\text{dsub}}$ is a non-convex QCQP-1 problem similar to $\mathcal{P}_{\text{dsub}}(\mathbf{v})$. Thus, with a procedure similar to that in Appendix A, we have the closed-form optimal solution \mathbf{d}_{ik} to $\mathcal{P}'_{\text{dsub}}$ given by

$$d_{jik}^o = \begin{cases} \frac{\tilde{e}_{1,iik}^{(n)}}{1 - \mu_{ik}^o} & \text{if } j = i, \\ \frac{\tilde{e}_{1,jik}^{(n)}}{1 + \mu_{ik}^o \gamma_{ik}} & \text{otherwise.} \end{cases}$$

where $\mu_{ik}^o = 0$ if $\gamma_{ik} \sum_{j \neq i} |\tilde{e}_{1,jik}^{(n)}|^2 + \gamma_{ik} \sigma^2 - |\tilde{e}_{1,iik}^{(n)}|^2 \leq 0$; otherwise the following quartic equation is guaranteed to have a unique root in $(0, 1)$, and μ_{ik}^o is this unique root:

$$\gamma_{ik} \frac{\sum_{j \neq i} |\tilde{e}_{1,jik}^{(n)}|^2}{(1 + \mu_{ik}^o \gamma_{ik})^2} + \gamma_{ik} \sigma^2 - \frac{|\tilde{e}_{1,iik}^{(n)}|^2}{(1 - \mu_{ik}^o)^2} = 0.$$

2) *Closed-Form a-update in (32)*: Given $\mathbf{d}^{(n+1)}$ and $\tilde{\mathbf{q}}^{(n)}$, the optimization problem in (32) can be decomposed into G subproblems, one for each group j given by

$$\mathcal{P}'_{\text{asub}} : \min_{\mathbf{a}} \sum_{i=1}^G \sum_{k=1}^{K_i} |d_{jik}^{(n+1)} - \mathbf{a}_j^H \mathbf{f}_{jik} + \tilde{q}_{jik}^{(n)}|^2,$$

which is an unconstrained quadratic convex optimization problem. The closed-form solution to $\mathcal{P}'_{\text{asub}}$ is expressed as

$$\mathbf{a}_j^{(n+1)} = \left(\sum_{i=1}^G \sum_{k=1}^{K_i} \mathbf{f}_{jik} \mathbf{f}_{jik}^H \right)^{-1} \sum_{i=1}^G \sum_{k=1}^{K_i} \left(d_{jik}^{(n+1)} + \tilde{q}_{jik}^{(n)} \right)^* \mathbf{f}_{jik}.$$

APPENDIX C PROOF OF PROPOSITION 1

Proof: It is straightforward to check that the scaled beamforming vector $\mathbf{w}^s(\gamma, P) = \sqrt{\frac{P}{P^Q(\gamma)}} \mathbf{w}^Q(\gamma)$ satisfies constraint (2) and therefore is a feasible solution to $\mathcal{S}_o(\gamma, P)$. The achieved objective value $t^s(\gamma, P)$ corresponding to $\mathbf{w}^s(\gamma, P)$ is expressed in terms of $\mathbf{w}^Q(\gamma)$ as

$$\begin{aligned} t^s(\gamma, P) &= \min_{i,k} \frac{1}{\gamma_{ik}} \frac{\frac{P}{P^Q(\gamma)} |\mathbf{h}_{ik}^H \mathbf{w}_i^Q(\gamma)|^2}{\frac{P}{P^Q(\gamma)} I_{ik}^Q(\gamma) + \sigma^2} \\ &= \min_{i,k} \frac{\frac{P}{P^Q(\gamma)} |\mathbf{h}_{ik}^H \mathbf{w}_i^Q(\gamma)|^2}{\gamma_{ik} I_{ik}^Q(\gamma) + \gamma_{ik} \sigma^2} \frac{I_{ik}^Q(\gamma) + \sigma^2}{\frac{P}{P^Q(\gamma)} I_{ik}^Q(\gamma) + \sigma^2}. \end{aligned} \quad (37)$$

Define $t^Q(\gamma) \triangleq \min_{i,k} \frac{|\mathbf{h}_{ik}^H \mathbf{w}_i^Q(\gamma)|^2}{\gamma_{ik} I_{ik}^Q(\gamma) + \gamma_{ik} \sigma^2}$. Since $\mathbf{w}^Q(\gamma)$ satisfies constraint (1) in $\mathcal{P}_o(\gamma)$ as a feasible solution, we have $\frac{|\mathbf{h}_{ik}^H \mathbf{w}_i^Q(\gamma)|^2}{I_{ik}^Q(\gamma) + \sigma^2} \geq \gamma_{ik}$ for $k \in \mathcal{K}_i$, $i \in \mathcal{G}$. It follows that $t^Q(\gamma) \geq 1$.

Based on this, from (37), we have

$$\begin{aligned} t^s(\gamma, P) &\geq \frac{P}{P^Q(\gamma)} t^Q(\gamma) \min_{i,k} \frac{I_{ik}^Q(\gamma) + \sigma^2}{\frac{P}{P^Q(\gamma)} I_{ik}^Q(\gamma) + \sigma^2} \\ &\geq \frac{P}{P^Q(\gamma)} \min_{i,k} \frac{I_{ik}^Q(\gamma) + \sigma^2}{\frac{P}{P^Q(\gamma)} I_{ik}^Q(\gamma) + \sigma^2}. \end{aligned} \quad (38)$$

From (37), we can also obtain an upper bound on $t^s(\gamma, P)$ as

$$\begin{aligned} t^s(\gamma, P) &\leq \frac{P}{P^Q(\gamma)} t^Q(\gamma) \frac{I_{i'k'}^Q(\gamma) + \sigma^2}{\frac{P}{P^Q(\gamma)} I_{i'k'}^Q(\gamma) + \sigma^2} \\ &\leq \frac{P}{P^Q(\gamma)} t^Q(\gamma) \max_{i,k} \frac{I_{ik}^Q(\gamma) + \sigma^2}{\frac{P}{P^Q(\gamma)} I_{ik}^Q(\gamma) + \sigma^2} \end{aligned} \quad (39)$$

where $\{i', k'\} = \arg \min_{i,k} \frac{|\mathbf{h}_{ik}^H \mathbf{w}_i^Q(\gamma)|^2}{\gamma_{ik} I_{ik}^Q(\gamma) + \gamma_{ik} \sigma^2}$. Note that the scaled beamforming vector $\frac{\mathbf{w}_i^Q(\gamma)}{\sqrt{t^Q(\gamma)}}$ results in the transmit power $\frac{P^Q(\gamma)}{t^Q(\gamma)}$.

Then, with $\frac{P^Q(\gamma)}{\sqrt{t^Q(\gamma)}}$, the achieved weighted SINR, for any $k \in \mathcal{K}_i, i \in \mathcal{G}$, is given by

$$\frac{1}{\gamma_{ik}} \frac{1}{t^Q(\gamma)} \frac{|\mathbf{h}_{ik}^H \mathbf{w}_i^Q(\gamma)|^2}{I_{ik}^Q(\gamma) + \sigma^2} \stackrel{(a)}{\geq} \frac{1}{\gamma_{ik} t^Q(\gamma)} \frac{|\mathbf{h}_{ik}^H \mathbf{w}_i^Q(\gamma)|^2}{I_{ik}^Q(\gamma) + \sigma^2} \stackrel{(b)}{\geq} 1 \quad (40)$$

where (a) is due to $t^Q(\gamma) \geq 1$, and (b) is from the definition of $t^Q(\gamma)$. Thus, the beamforming vector $\frac{\mathbf{w}_i^Q(\gamma)}{\sqrt{t^Q(\gamma)}}$ is feasible to $\mathcal{P}_o(\gamma)$ and $\frac{P^Q(\gamma)}{t^Q(\gamma)} \geq P^o(\gamma)$, where $P^o(\gamma)$ is the minimum transmit power in $\mathcal{P}_o(\gamma)$. Applying $\frac{P^Q(\gamma)}{t^Q(\gamma)} \geq P^o(\gamma)$ to the RHS of (39) yields

$$t^s(\gamma, P) \leq \frac{P}{P^o(\gamma)} \max_{i,k} \frac{I_{ik}^Q(\gamma) + \sigma^2}{\frac{P}{P^o(\gamma)} I_{ik}^Q(\gamma) + \sigma^2}. \quad (41)$$

Combining (38) and (41), we have (35). ■

REFERENCES

- [1] C. Zhang, M. Dong, and B. Liang, "First-order fast algorithm for structurally optimal multi-group multicast beamforming in large-scale systems," in *IEEE ICASSP*, June 2021, pp. 4790–4794.
- [2] M. Dong and Q. Wang, "Multi-group multicast beamforming: Optimal structure and efficient algorithms," *IEEE Trans. Signal Process.*, vol. 68, pp. 3738–3753, May 2020.
- [3] E. G. Larsson, O. Edfors, F. Tufvesson, and T. L. Marzetta, "Massive MIMO for next generation wireless systems," *IEEE Commun. Mag.*, vol. 52, no. 2, pp. 186–195, Feb. 2014.
- [4] N. D. Sidiropoulos, T. N. Davidson, and Z.-Q. Luo, "Transmit beamforming for physical-layer multicasting," *IEEE Trans. Signal Process.*, vol. 54, no. 6, pp. 2239–2251, Jun. 2006.
- [5] E. Karipidis, N. D. Sidiropoulos, and Z.-Q. Luo, "Quality of service and max-min fair transmit beamforming to multiple cochannel multicast groups," *IEEE Trans. Signal Process.*, vol. 56, no. 3, pp. 1268–1279, Mar. 2008.
- [6] D. Christopoulos, S. Chatzinotas, and B. Ottersten, "Weighted fair multicast multigroup beamforming under per-antenna power constraints," *IEEE Trans. Signal Process.*, vol. 62, no. 19, pp. 5132–5142, Oct. 2014.
- [7] M. Jordan, X. Gong, and G. Ascheid, "Multicell multicast beamforming with delayed SNR feedback," in *IEEE GLOBECOM*, Nov. 2009, pp. 1–6.
- [8] Z. Xiang, M. Tao, and X. Wang, "Coordinated multicast beamforming in multicell networks," *IEEE Trans. Wireless Commun.*, vol. 12, no. 1, pp. 12–21, Jan. 2013.
- [9] N. Bornhorst, M. Pesavento, and A. B. Gershman, "Distributed beamforming for multi-group multicasting relay networks," *IEEE Trans. Signal Process.*, vol. 60, no. 1, pp. 221–232, Jan. 2012.
- [10] M. Dong and B. Liang, "Multicast relay beamforming through dual approach," in *IEEE CAMSAP*, Dec. 2013, pp. 492–495.
- [11] K. T. Phan, S. A. Vorobyov, N. D. Sidiropoulos, and C. Tellambura, "Spectrum sharing in wireless networks via QoS-aware secondary multicast beamforming," *IEEE Trans. Signal Process.*, vol. 57, no. 6, pp. 2323–2335, June 2009.
- [12] Y. Huang, Q. Li, W.-K. Ma, and S. Zhang, "Robust multicast beamforming for spectrum sharing-based cognitive radios," *IEEE Trans. Signal Process.*, vol. 60, no. 1, pp. 527–533, Jan. 2012.
- [13] Z.-Q. Luo, W.-K. Ma, A. M.-C. So, Y. Ye, and S. Zhang, "Semidefinite relaxation of quadratic optimization problems," *IEEE Signal Process. Mag.*, vol. 27, no. 3, pp. 20–34, May 2010.
- [14] B. R. Marks and G. P. Wright, "A general inner approximation algorithm for nonconvex mathematical programs," *Oper. Res.*, vol. 26, no. 4, pp. 681–683, Aug. 1978.
- [15] L. Tran, M. F. Hanif, and M. Juntti, "A conic quadratic programming approach to physical layer multicasting for large-scale antenna arrays," *IEEE Signal Process. Lett.*, vol. 21, no. 1, pp. 114–117, Jan. 2014.
- [16] O. Mehanna, K. Huang, B. Gopalakrishnan, A. Konar, and N. D. Sidiropoulos, "Feasible point pursuit and successive approximation of non-convex QCQPs," *IEEE Signal Process. Lett.*, vol. 22, no. 7, pp. 804–808, Jul. 2015.
- [17] D. Christopoulos, S. Chatzinotas, and B. Ottersten, "Multicast multigroup beamforming for per-antenna power constrained large-scale arrays," in *IEEE SPAWC*, June 2015, pp. 271–275.
- [18] S. Boyd and L. Vandenberghe, *Convex Optimization*, Cambridge, U.K.: Cambridge Univ. Press, 2004.
- [19] A. Konar and N. D. Sidiropoulos, "Fast approximation algorithms for a class of non-convex QCQP problems using first-order methods," *IEEE Trans. Signal Process.*, vol. 65, no. 13, pp. 3494–3509, Jul. 2017.
- [20] M. S. Ibrahim, A. Konar, and N. D. Sidiropoulos, "Fast algorithms for joint multicast beamforming and antenna selection in massive MIMO," *IEEE Trans. Signal Process.*, vol. 68, pp. 1897–1909, Mar. 2020.
- [21] E. Chen and M. Tao, "ADMM-based fast algorithm for multi-group multicast beamforming in large-scale wireless systems," *IEEE Trans. Commun.*, vol. 65, no. 6, pp. 2685–2698, Jun. 2017.
- [22] M. Sadeghi, L. Sanguinetti, R. Couillet, and C. Yuen, "Reducing the computational complexity of multicasting in large-scale antenna systems," *IEEE Trans. Wireless Commun.*, vol. 16, no. 5, pp. 2963–2975, May 2017.
- [23] J. Yu and M. Dong, "Low-complexity weighted MRT multicast beamforming in massive MIMO cellular networks," in *IEEE ICASSP*, Apr. 2018, pp. 3849–3853.
- [24] J. Yu and M. Dong, "Distributed low-complexity multi-cell coordinated multicast beamforming with large-scale antennas," in *IEEE SPAWC*, June 2018, pp. 1–5.
- [25] Z. Xiang, M. Tao, and X. Wang, "Massive MIMO multicasting in noncooperative cellular networks," *IEEE J. Sel. Areas Commun.*, vol. 32, no. 6, pp. 1180–1193, June 2014.
- [26] M. Sadeghi and C. Yuen, "Multi-cell multi-group massive MIMO multicasting: An asymptotic analysis," in *IEEE GLOBECOM*, Dec. 2015, pp. 1–6.
- [27] O. Tervo, L. Tran, H. Pennanen, S. Chatzinotas, B. Ottersten, and M. Juntti, "Energy-efficient multicell multigroup multicasting with joint beamforming and antenna selection," *IEEE Trans. Signal Process.*, vol. 66, no. 18, pp. 4904–4919, Sept. 2018.
- [28] M. Sadeghi, E. Björnson, E. G. Larsson, C. Yuen, and T. Marzetta, "Joint unicast and multi-group multicast transmission in massive MIMO systems," *IEEE Trans. Wireless Commun.*, vol. 17, no. 10, pp. 6375–6388, Oct. 2018.
- [29] S. Mohammadi, M. Dong, and S. ShahbazPanahi, "Fast algorithm for joint unicast and multicast beamforming in large-scale systems," in *IEEE SPAWC*, Sept. 2021, pp. 91–95.
- [30] H. Joudeh and B. Clerckx, "Rate-splitting for max-min fair multigroup multicast beamforming in overloaded systems," *IEEE Trans. Wireless Commun.*, vol. 16, no. 11, pp. 7276–7289, Nov. 2017.
- [31] O. Tervo, L.-N. Tran, S. Chatzinotas, B. Ottersten, and M. Juntti, "Multi-group multicast beamforming and antenna selection with rate-splitting in multicell systems," in *IEEE SPAWC*, June 2018, pp. 1–5.
- [32] H. Chen, D. Mi, B. Clerckx, Z. Chu, J. Shi, and P. Xiao, "Joint power and subcarrier allocation optimization for multigroup multicast systems with rate splitting," *IEEE Trans. Veh. Technol.*, vol. 69, no. 2, pp. 2306–2310, Feb. 2020.
- [33] F. Facchinei and J.-S. Pang, *Finite-Dimensional Variational Inequalities and Complementarity Problems*, New York, NY: Springer-Verlag, 2003.
- [34] G. M. Korpelevich, "The extragradient method for finding saddle points and other problems," *Matecon*, vol. 13, pp. 35–49, 1977.
- [35] E. N. Khotobov, "Modification of the extra-gradient method for solving variational inequalities and certain optimization problems," *USSR Comput. Math. Math. Phys.*, vol. 27, no. 5, pp. 120–127, 1987.
- [36] P. Marcotte, "Application of Khotobov's algorithm to variational inequalities and network equilibrium problems," *Inf. Syst. Oper. Res.*, vol. 29, no. 4, pp. 258–270, Nov. 1991.
- [37] S. Boyd, N. Parikh, E. Chu, B. Peleato, and J. Eckstein, "Distributed optimization and statistical learning via the alternating direction method of multipliers," *Found. Trends Mach. Learn.*, vol. 3, no. 1, pp. 1–122, 2011.